AN ABSTRACT OF THE THESIS OF

RICHARD DENNIS KNARR for the M.S. in CHEMISTRY
(Name) (Degree) (Major)

Date thesis is presented November 22, 1966

Title THE DESIGN AND EVALUATION OF A RECORDING CONDUCTOMETRIC TITRATOR

Abstract approved Redacted for Privacy
(Major professor)

A Heath EUW-20A Servo-Recorder was converted to a self-balancing, recording Wheatstone bridge. The EUW-20A 1000Ω slide-wire was used as the variable resistance arm of the bridge, the servo-amplifier was used as the bridge unbalance signal detector, and the servo-motor was used to balance the bridge automatically. The bridge was arranged to produce a readout directly proportional to the conductance of the measured element.

The problems accompanying the measurement of electrolytic conductance with this instrument were identified. There are two major sets of problems: Those arising from adverse cell conditions involving stirring rate, electrolyte concentration and electrode condition, and those arising from cell capacitance associated with the ionic double-layer at the electrodes. The cell capacitance causes a phase difference between the a-c potentials of two of the bridge arms. This phase difference causes a significant dead band in the recorder response.

Two sets of conductometric titrations of Na_2CO_3 with HCl were performed, one using a sine wave to excite the bridge and one using a square wave. The error in the results obtained from these titrations was generally less than one percent and the reproducibility was one-half percent or less. The instrument performed satisfactorily when the conductance change occurring during the titration was as low as five percent.

THE DESIGN AND EVALUATION OF A RECORDING CONDUCTOMETRIC TITRATOR

by

RICHARD DENNIS KNARR

A THESIS

submitted to

OREGON STATE UNIVERSITY

in partial fulfillment of
the requirements for the
degree of

MASTER OF SCIENCE

June 1967

APPROVED:

Redacted for Privacy

Professor of Chemistry
In Charge of Major

Redacted for Privacy

Head of Department of Chemistry

Redacted for Privacy

Dean of Graduate School

Date thesis is presented November 22, 1966

Typed by Gwendolyn Hansen

ACKNOWLEDGMENT

The author wishes to acknowledge the contributions made to this project by several people. Dr. Harry Freund supervised and directed the work. Dr. Harold McBride, working on the Faculty Research Participation Program sponsored by the national Science Foundation during the summers of 1964 and 1965, laid the foundation for this investigation by modifying the Heath EUW-20A to serve as a conductometric CO_2 monitor. The author's wife, Marlene, gave encouragement and clerical help during the crucial periods of this project.

TABLE OF CONTENTS

LIST OF FIGURES

Figure		Page

LIST OF TABLES

THE DESIGN AND EVALUATION OF A RECORDING CONDUCTOMETRIC TITRATOR

INTRODUCTION

Objective of the Study

Although the phenomenon of electrolytic conductance has been known and understood for many years, it has been used sparingly as an endpoint indicator for titrations. The use of conductance behavior as an indicator has two advantages over other indicators. First, conductance can be used in colored or opaque systems, and second, conductance can be used in any system which is accompanied by a change in conductance, i.e., it is sensitive to many different ionic species. There are also two disadvantages to this method. First, the measured conductance is the total conductance of all the ionic species in the solution. Therefore, if the ion of interest contributes only a small fraction of the total conductance, its reaction with a titrant will cause only a small change in conductance. Any measuring instrument must then be able to detect a small conductance change. Second, the instrument traditionally used, the conventional Wheatstone bridge, makes each titration time-consuming. The titrant must be added in increments, the conductance measured after each increment, the results plotted on a graph of conductance versus volume of titrant, and the resulting straight lines extrapolated to their intersection at the endpoint.

The first disadvantage can be overcome only by the creation of increasingly sensitive instruments. The second can be eliminated by adding the titrant at a constant rate and measuring the conductance with a recording instrument. The purpose of this study is to investigate the feasibility of using a self-balancing, recording Wheatstone bridge for conductometric titrations.

Theory of Electrolytic Conductance (11)

The resistance of any conductor varies directly with its length and inversely with its cross-sectional area, i.e.,

$$R = \rho \; l/A \tag{1}$$

where R is the resistance in ohms, l is the length in centimeters and A is the cross-sectional area in square centimeters. ρ is a constant which is a characteristic property of the conductor and is called the specific resistivity. It can be seen from equation (1) that ρ is the resistance of a section of the conductor having a length of 1 centimeter and a cross-sectional area of 1 square centimeter. From equation (1) it is clear that the expression for the corresponding conductance, L, is

$$\begin{aligned} L &= 1/R = 1/\rho \; (A/l) \\ &= L_s (A/l) \end{aligned} \tag{2}$$

where $L_s = 1/\rho$ is the specific conductance of the conductor, and is expressed in units of reciprocal ohms or mhos. L_s may be considered the conductance of a cube of material one centimeter on a side.

If C is the concentration of a solution in equivalents per liter, then $C/1000$ is the concentration per cubic centimeter, and the volume containing one equivalent of the solute is $1000/C$ cubic centimeters. Since L_s is the conductance of a centimeter cube of solution, the conductance of $1000/C$ cubic centimeters is $1000L_s/C$ when the solution is placed between two parallel electrodes one centimeter apart and large enough to contain all the solution between them. The equation:

$$\Lambda = 1000L_s/C \tag{3}$$

defines the equivalent conductance, Λ.

According to equation (2),

$$L_s = (1/A)L = (1/A)1/R \tag{4}$$

Before L_s for any electrolyte can be calculated from the measured value of R, the ratio $1/A$ must be known. This ratio is a fixed property of the particular cell used and is independent of the elecrolyte used and of its concentration. The ratio $1/A$ is called the cell constant, θ. θ is not evaluated by measuring the length and area of the electrodes because they are usually surrounded by solution making measurement of the effective area difficult, and are often of shapes that are difficult to measure. Instead, a solution of known L_s is placed in the cell, R is measured, and θ is calculated from equation (4) in the form:

$$L_s = \theta/R \tag{5}$$

The form of these relationships used in conductometric titrations is obtained by substituting (5) into (3) and rearranging. Thus,

$$\Lambda = \frac{1000\theta/R}{C}$$

$$1/R = \frac{1}{1000\theta} \Lambda C \tag{6}$$

Since the conductance of a solution is the sum of the conductances of all its ions, equation (6) becomes

$$1/R = \frac{1}{1000\theta} \Sigma \Lambda_i C_i \tag{7}$$

where the subscript i refers to a particular ion. From equation (7) it is clear that the measured conductance of a solution is directly proportional to the concentration of solute.

As an example of the conductance changes during a titration, consider the titration of 0.1N NaOH with 1.N HCl. The following equivalent ionic conductances are used:

$$H^+ = 349.82 \text{ mho cm}^{-1} \text{ equiv.}^{-1}$$

$$Na^+ = 50.11 \text{ mho cm}^{-1} \text{ equiv.}^{-1}$$

$$OH^- = 198 \text{ mho cm}^{-1} \text{ equiv.}^{-1}$$

$$Cl^- = 76.34 \text{ mho cm}^{-1} \text{ equiv.}^{-1}$$

If the cell constant is one, the conductance at the beginning of the titration is, from equation (7), 0.248 mho. At the endpoint, neglecting dilution, the solution will be 0.1 N NaCl with a conductance of 0.126 mho. After the endpoint, the concentration of H^+, with a Λ of 349.82 increases rapidly and pushes the solution conductance up. Therefore, the graph of conductance versus ml of titrant starts at a high conductance level, decreases by nearly 50% to the endpoint, then increases. A chart of this titration is shown in Figure 1.

While it is true that the equivalent conductance varies with concentration, this effect is small enough to be neglected in titrations. In a conductometric titration it is not necessary to know the conductance of the solution, only the point on the graph of conductance versus volume of titrant at which the rate of change of conductance changes, i.e., the point at which the slope of the line changes. This point signifies the endpoint of the titration.

Instrumentation

The traditional instrument used in conductometric titrations is the Wheatstone bridge, which will be discussed in a later section.

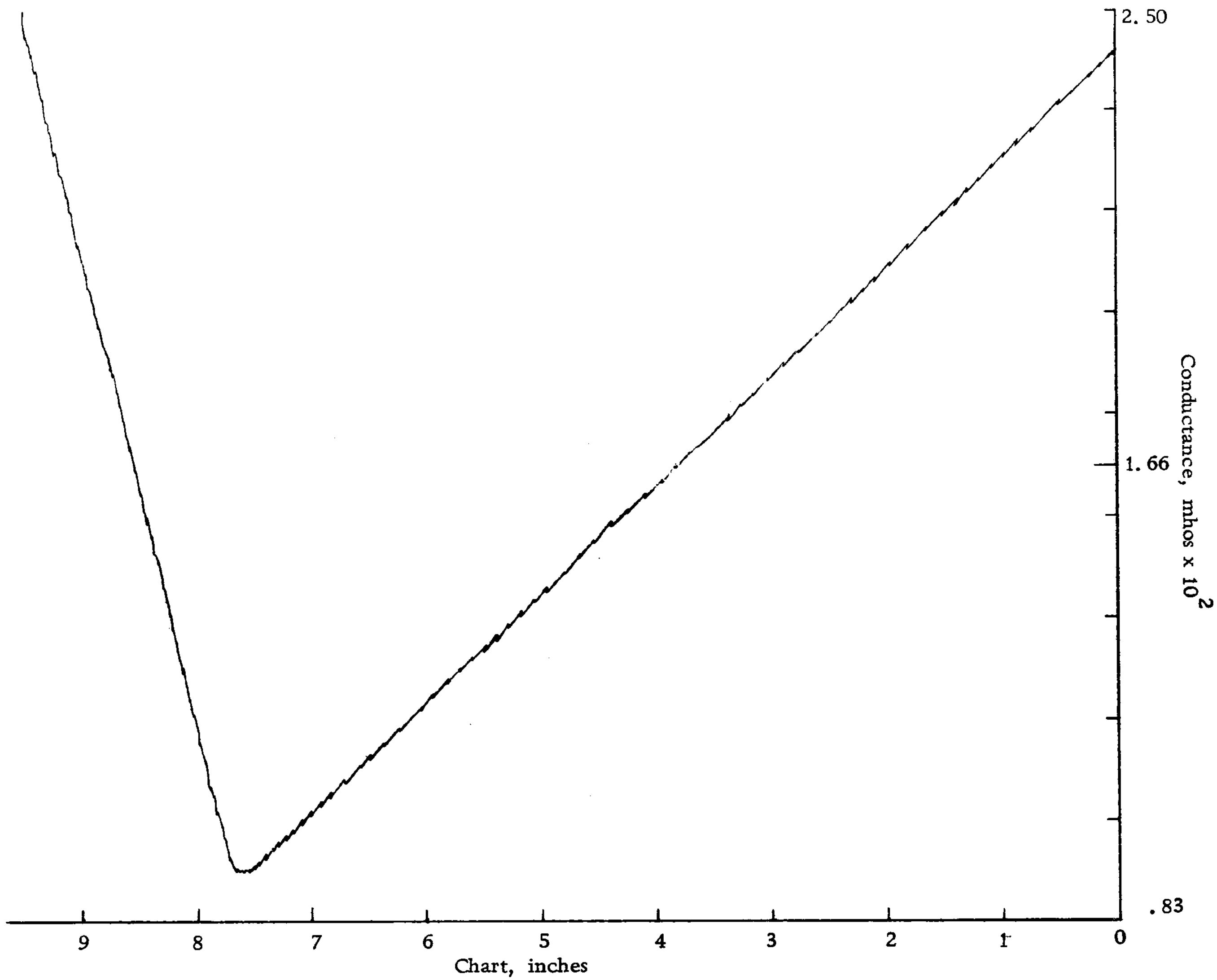

Figure 1. Conductometric titrator of 0.1 N NaOH with 1 N HCl

Recently, several instruments have been described (1, 2, 3, 6, 7, 9, 13) which utilize a principle different from the Wheatstone bridge. These instruments all place an impedance in series with the titration cell and measure the IR drop across that impedance. Since R is constant, the variation in IR drop must be a function of I, and I is determined by the total resistance of the circuit. As the conductance of the cell varies during the titration, the value of I varies proportionally and so does the value of the IR drop. This type of instrument is shown schematically in Figure 2. The disadvantages of this type instrument are that it needs a very stable voltage source to keep the voltage across the entire circuit constant, and that the value of R must be very small compared to the cell impedance so that the current in the circuit will be an accurate reflection of the cell conductance. Some authors (4, 11, 12) used operational amplifier instruments which deliver high sensitivity and linear conductance readout, but which need very stable power supplies and other components for satisfactory operation. Only one paper (13) described a self-balancing Wheatstone bridge used for conductometric titration, and that instrument is not automatic recording.

Thus, it appears that a self-balancing, automatic recording Wheatstone bridge fills the need for a relatively simple, inexpensive, rugged, dependable instrument.

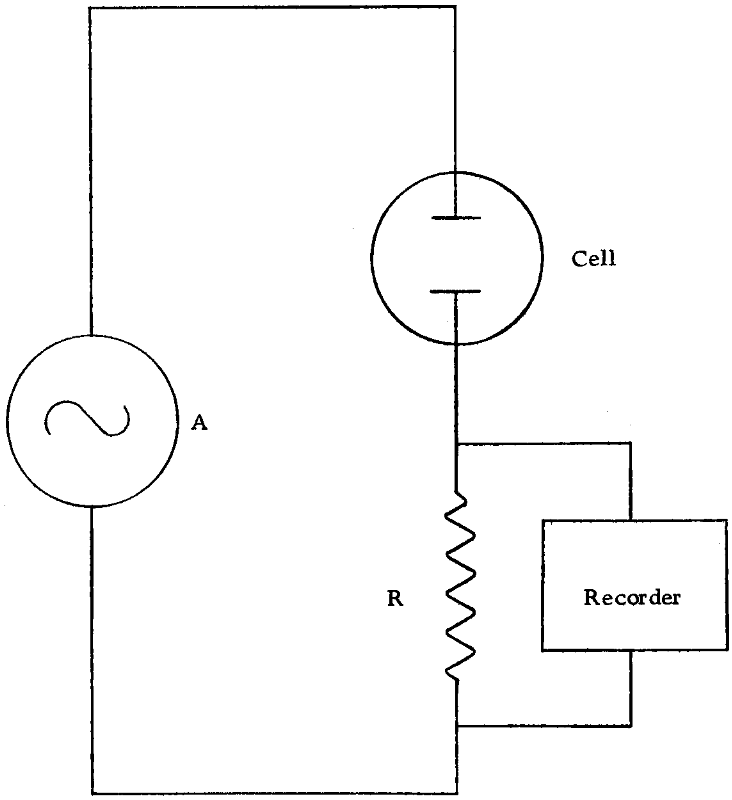

Figure 2. Conductance Monitor. R is a resistance small when compared with the cell resistance. A is a source of alternating current.

EXPERIMENTAL

Description of the Instrument

Elementary Wheatstone Bridge Analysis

The analysis of a Wheatstone bridge composed of purely resistive elements, such as the one shown in Figure 3, can be performed by considering the bridge to be two voltage dividers. Thus, the voltage at point 1, referred to point 3, is given by

$$e_1 = E\ R_2/(R_1 + R_2) \tag{8}$$

Similarly, the voltage at point 2 is given by

$$e_2 = E\ R_4/(R_3 + R_4) \tag{9}$$

When the bridge is balanced, $e_1 = e_2$ and the right sides of (8) and (9) can be set equal to each other:

$$E\ R_2/(R_1 + R_2) = E\ R_4/(R_3 + R_4) \tag{10}$$

Canceling E's and cross-multiplying gives

$$R_2R_3 + R_2R_4 = R_1R_4 + R_2R_4 \tag{11}$$

Subtracting R_2R_4 from each side and rearranging gives

$$R_3/R_4 = R_1/R_2 \tag{12}$$

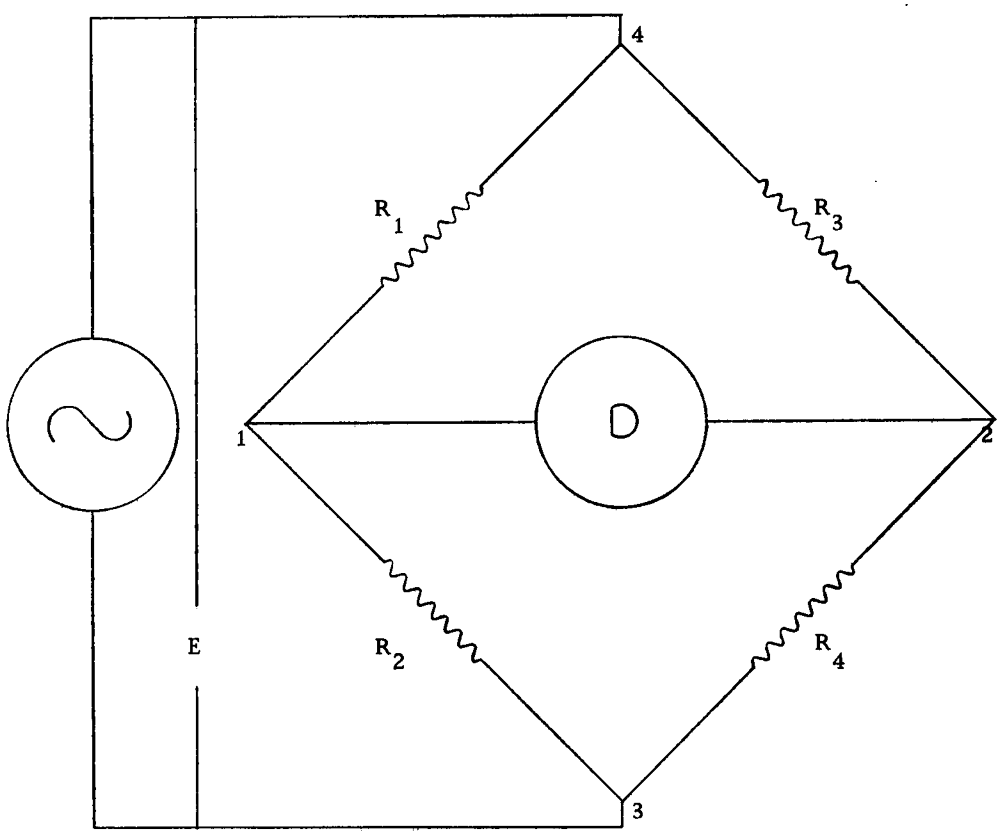

Figure 3. Wheatstone bridge composed of pure resistances.

the familiar bridge-balance equation. Strictly speaking, the resistances involved should be called impedances since this is an a-c system, but there are no reactive properties associated with pure resistances, so the above treatment yields a valid result.

If the bridge of Figure 3 were used to measure resistance, the unknown resistance would be R_3 and the variable resistance would be R_4. The relationship between R_3 and R_4 is obtained by rearranging equation (12) as follows:

$$R_4 = (R_2/R_1)\,R_3 \tag{13}$$

Thus, the variable resistance, R_4, is directly proportional to the unknown resistance, R_3. Such a resistance bridge could be and has been used in the traditional point-by-point method of conductometric titration. The resistance values obtained were merely converted to conductance and plotted against volume of titrant.

A recording instrument, however, must provide a direct conductance readout. During a titration, the conductance of a solution often does not vary directly with volume of titrant added in the vicinity of the endpoint, because of hydrolysis effects. The endpoint must be located by extrapolating the linear portions of the conductance versus volume of titrant curve which were obtained before the endpoint region and after the endpoint was passed. The intersection of these lines is the point where the slope of the curve changes or the endpoint. Because resistance is the reciprocal of conductance, a plot of resistance versus volume of titrant would be not a straight line, but a curve and therefore difficult to extrapolate. To obtain the straight lines necessary for extrapolation then, a conductance readout from the instrument is needed.

The resistance bridge of Figure 3 can be easily converted to conductance readout by making R_2 the variable resistance. Equation (12) can then be rearranged to

$$R_2 = R_1 R_4 (1/R_3) \tag{14}$$

so that the resistance of R_2 is proportional to the conductance of R_3. In this project, the conductance cell, in which the titrations were carried out, was placed in the position of R_3 and the variable resistor was placed in the position of R_2.

To increase the sensitivity of any Wheatstone bridge, a resistor may be inserted in series with the variable resistor. The resistor used in this case was a 50 kΩ, 10-turn Helipot equipped with a Duodial. When this Helipot was set on one kΩ, a 50% decrease of conductance in the titration cell would produce a full scale deflection of the recorder pen, since the total resistance in the variable arm was two kΩ, and a full-scale pen deflection would reduce the total to one kΩ. In the same way, a Helipot setting of 50 kΩ would cause a full-scale pen deflection when the conductance decreased by two percent. In this thesis, sensitivity will mean the conductance change necessary to produce a full-scale pen deflection.

This conductance bridge was made automatic recording by feeding the unbalance signal between points 1 and 2 to a servo system which used the signal to adjust the variable resistor to the balance point. A pen which was attached mechanically to R_2 moved across a chart as R_2 was being varied and indicated the resistance value of R_2. The servo system used was the Heath Servo-Recorder Model EUW-20A.

Heath Servo-Recorder Model EUW-20A and Modifications

The Heath EUW-20A, when connected in its normal operating mode, is a self-balancing, recording potentiometer. Figure 4 is a simplified schematic of the input section of the instrument when connected normally. The input voltage is fed as shown to one contact of the 60 cps mechanical chopper. The second chopper contact is held at a reference voltage which is some fraction of the 1.36v available from a mercury cell. The voltage dividers which provide a fraction of the total cell voltage are not shown in Figure 4. When the input voltage and the reference voltage are at different levels, the chopper output is a 60 cps square wave, shown in Figure 5. This signal is fed, through a capacitor which blocks the d-c offset, to the amplifier input. The amplified signal goes to the control winding of

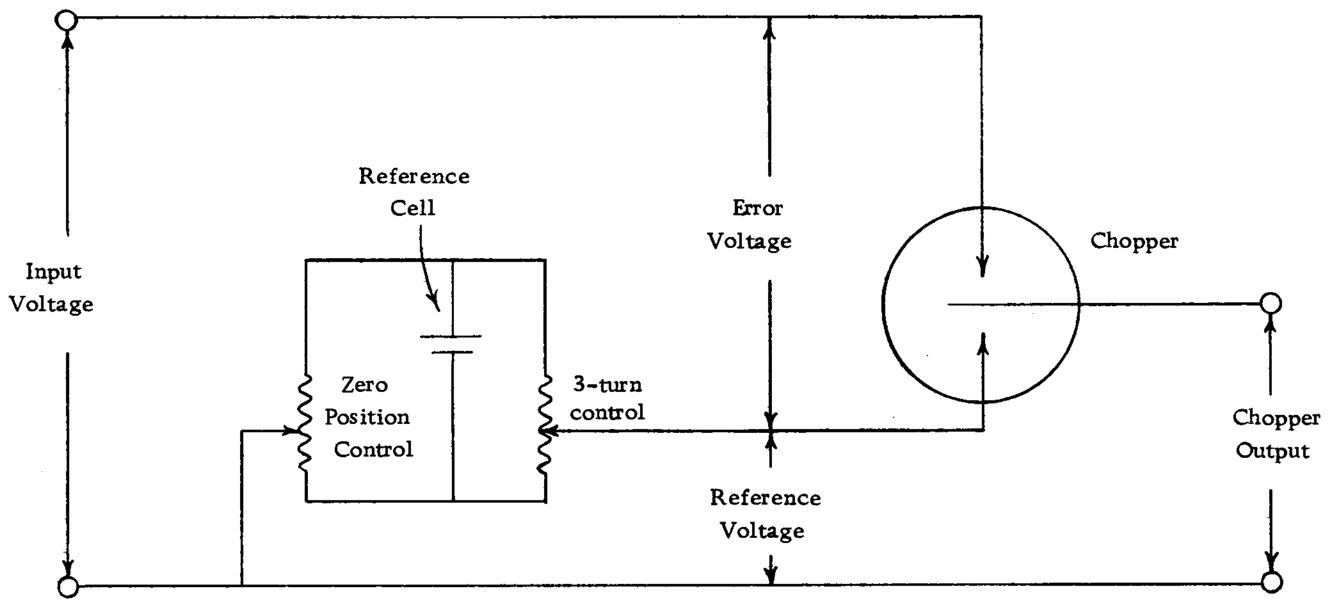

Figure 4. Simplified schematic of input section of Heath EUW-20A when used as a recording potentiometer (7).

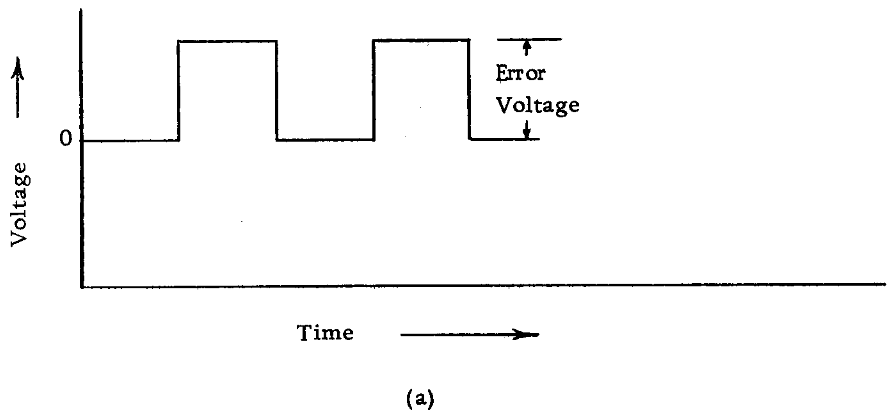

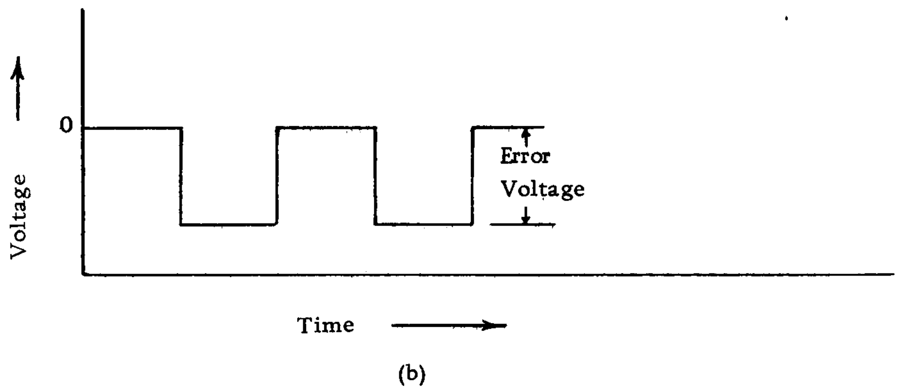

Figure 5. Chopper output signals (7).

the servomotor. As the servomotor turns, it moves the wiper of the 3-turn control. The reference voltage is thus adjusted until it is equal to the input voltage. If the input voltage is less than the reference voltage, the chopper output will be a square wave shifted 180° in phase from the previous square wave, as shown in Figure 5. In this case, the servomotor will turn the opposite direction from the previous case and will again balance the potentiometer.

In the amplifier are RC networks which shape the square wave into a distorted sine wave and shift it in phase by 90°. The 90° phase shift is necessary because the signal to the control winding of the servomotor must differ in phase by 90° from that at the reference winding (line voltage and phase) so that the necessary rotating magnetic field will occur. The chopper output signal will be either in phase or 180° out of phase with the line since the chopper is operated by a signal from the power transformer of the instrument. The 90° amplifier phase shift then puts the amplifier output 90° out of phase with line.

To convert the EUW-20A from a potentiometer to a self-balancing Wheatstone bridge, the input section can be bypassed and the unbalance signal from the bridge can be fed directly to the amplifier. If the 3-turn control pot is used as a variable resistor in the R_2 position in Figure 2, and the titration cell is used as R_3, the result is a self-balancing bridge with conductance readout. The

EUW-20A is well suited to this type of modification because the leads to the chopper, slidewire, amplifier and other components are brought to three 5-pin plugs in the back of the instrument. Normally, these plugs are interconnected through removable 5-pin sockets with the appropriate leads, resistors and capacitors to make the instrument a recording potentiometer. To modify the instrument the connecting sockets can be removed and the desired connections made.

The phase behavior of the bridge unbalance signal is as follows. Consider the bridge shown in Figure 6. The resistor designated S is the one which can be varied to balance the bridge and can assume resistance values from zero to 2R. When S has a value of R, the bridge is balanced and the signal at 1, e_1, is a sine wave as shown in Figure 7. The signal at 2, e_2, is also a sine wave, equal in magnitude to e_1. The unbalance signal, e_2-e_1, is zero as shown. Now when $S > R$, the bridge is unbalanced and e_1 has a larger magnitude than at balance. e_2 is the same as at balance, and $e_2 - e_1$ is shifted in phase 180° from E. When $S < R$, e_1 has a smaller magnitude than e_2 and $e_2 - e_1$ is in phase with E. Thus, as the bridge goes from one side of balance to the other, $e_2 - e_1$ undergoes a 180° phase shift. The phase behavior of the unbalance signal is shown in Figure 8a. The larger amplitude sine wave is the bridge excitation signal and the smaller is the unbalance signal. The top exposure shows the bridge on one side of balance,

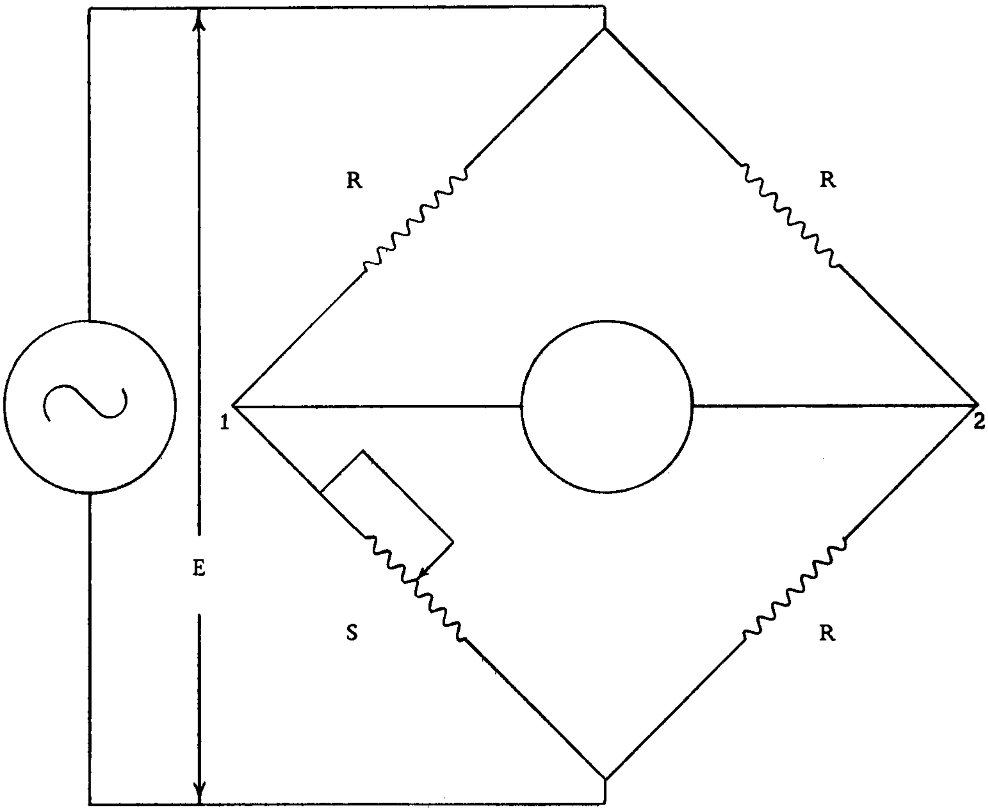

Figure 6. Wheatstone bridge for conductance measurements.

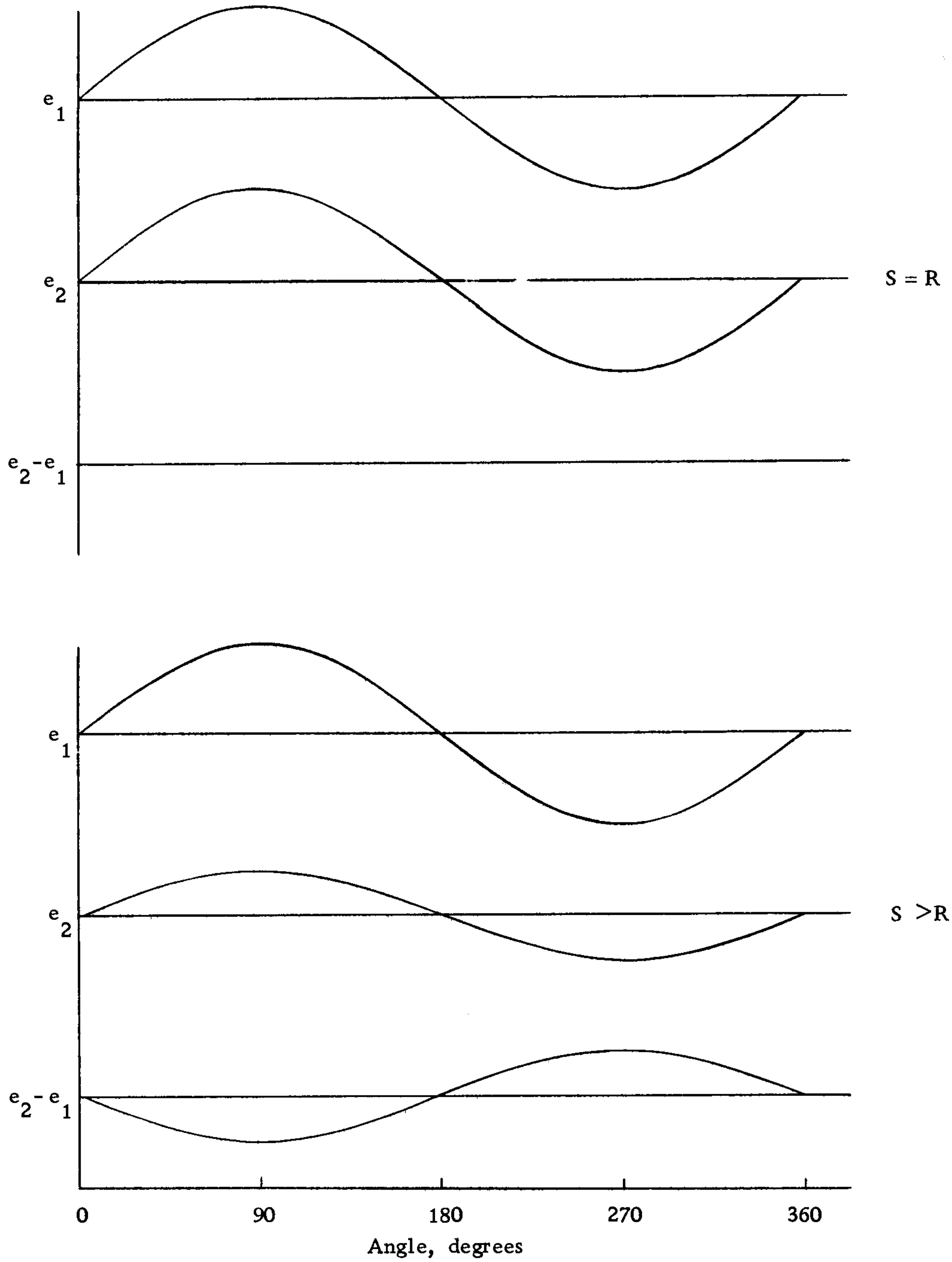

Figure 7. Conductance bridge signals.

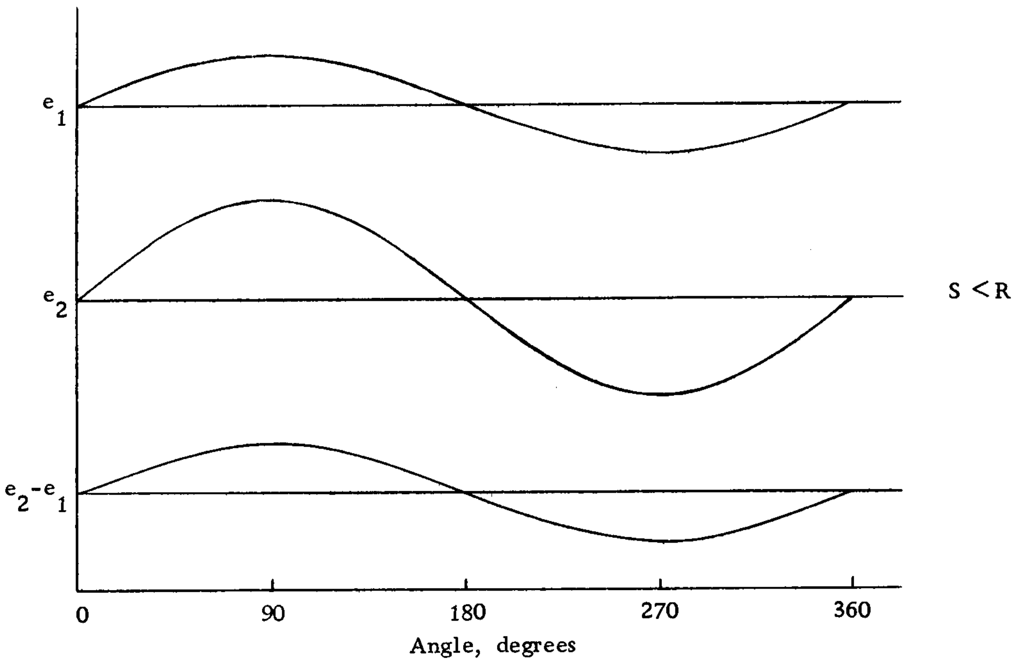

Figure 7. (Continued)

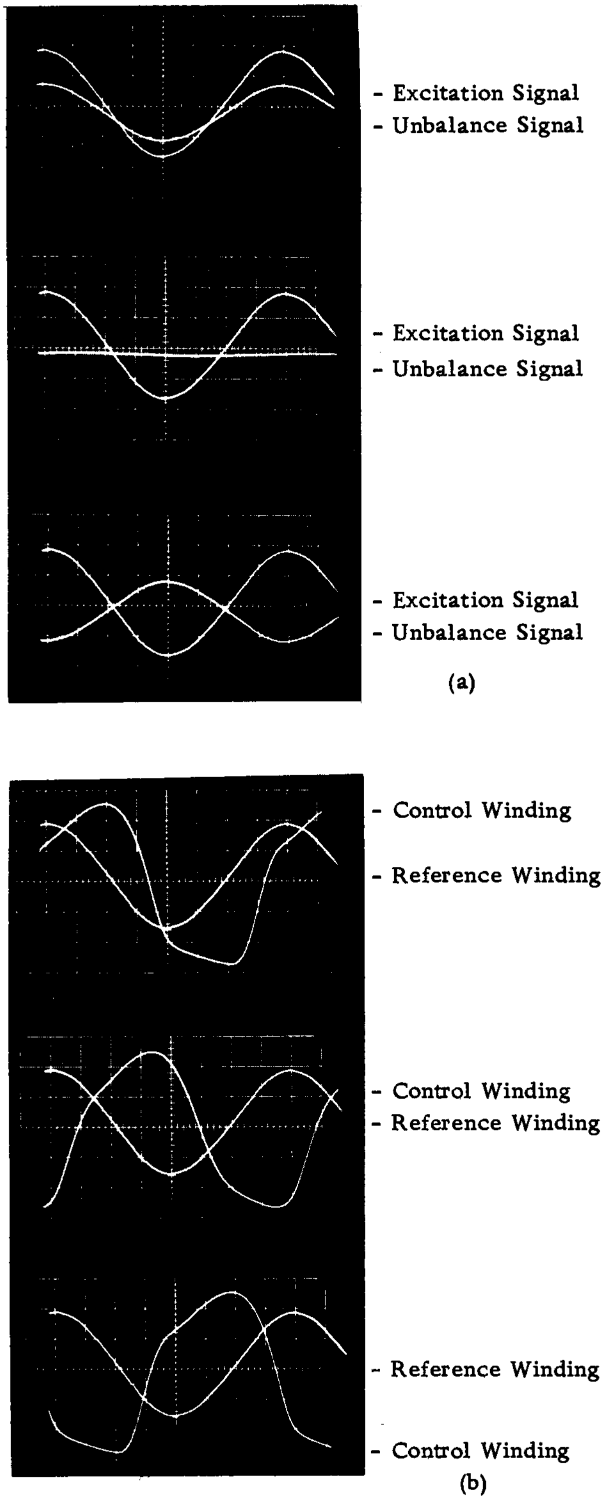

Figure 8. (a) Unbalance signals from resistive bridge
(b) amplifier outputs for (a).

the middle exposure at balance, and the bottom exposure on the other side of balance. In all the oscilloscope photos in this thesis, the sweep direction is from right to left. In all photos, each major horizontal grid division represents 45°. Figure 8b shows the amplifier outputs for the inputs shown in 8a. The output shown in the middle exposure is an amplifier hum, the cancellation of which is explained later. This shift in the amplifier input signal will result, as above, in a reversal of direction of the servomotor, and render the bridge self-balancing. The performance of this bridge as a conductance-measuring instrument is shown by the data presented in Figure 9.

To perform conductometric titrations, a titration vessel with stirring, a pair of electrodes to measure conductance and a system for delivering titrant at a constant rate are all needed. The vessel used was a standard 150 ml glass beaker with magnetic stirring. Six different sets of electrodes were tried with the final choice being blacked platinum wires 11 mm long, 2/3 mm in diameter and 30 mm apart in a vertical position. The reagent delivery system was a Manostat Digi-Pet, 10 ml size, driven by a Hurst reversible a-c motor equipped with a gear box to provide a six rpm output and an electrically operated clutch. When driven by a six rpm geared motor the Digi-Pet delivers approximately 1.85 ml of titrant per minute. The chart on the EUW-20A moves at a rate of two inches per minute.

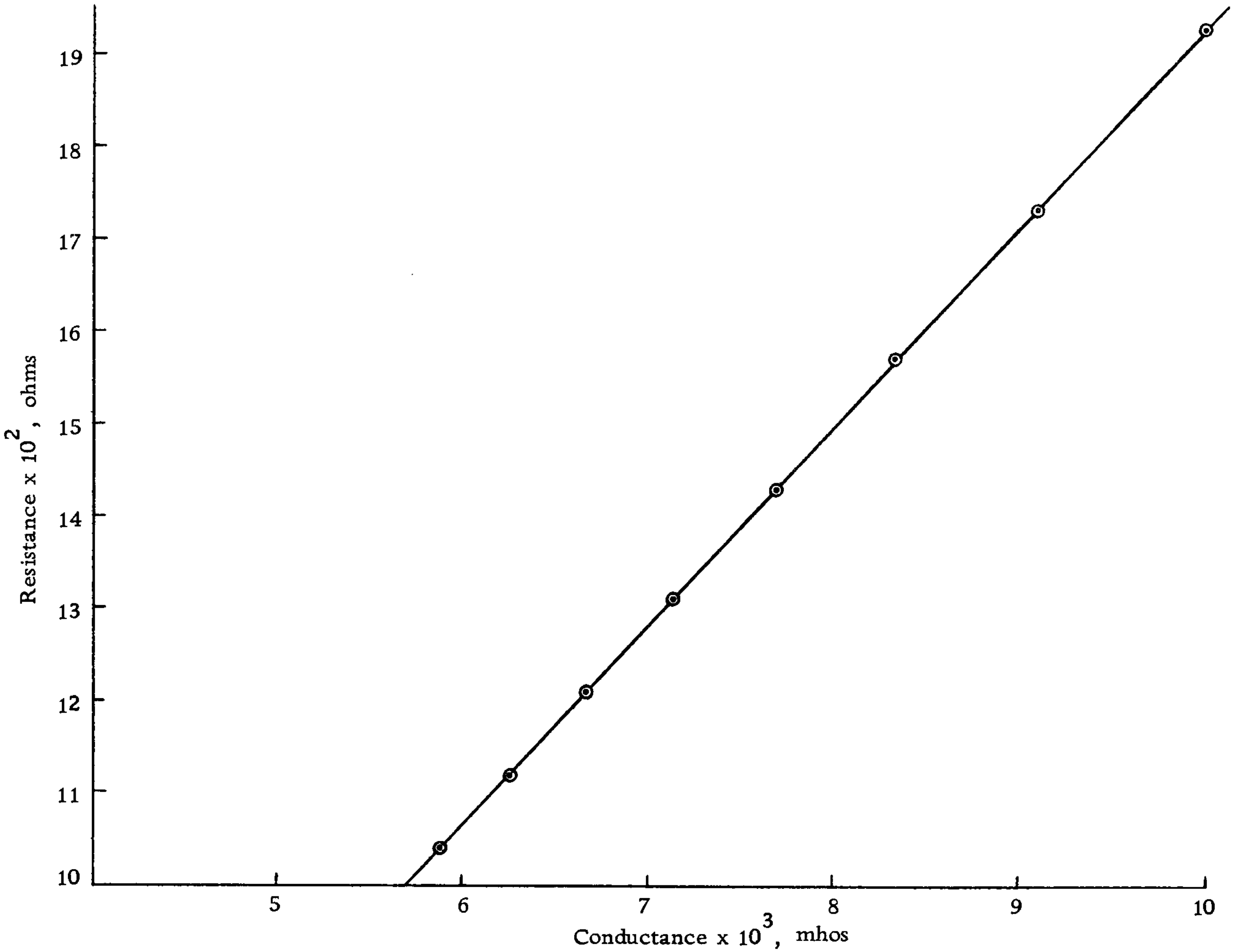

Figure 9. Unknown conductance versus slidewire resistance.

The relationship between titrant delivery rate and chart rate is therefore 0.925 ml per inch. The data from which this number was obtained are presented in Figure 10. The electrical switching arrangement used is shown schematically in Figure 11. The EUW-20A has two 115 v 60 cycle a-c outlets on the outside of its cabinet, one of which is activated when the instrument power switch is thrown to "Servo" and the other when the switch is thrown to "Chart." The power to operate the Digi-Pet is obtained from these outlets. When the "function" switch is in the left or "titrate" position, the motor is turning counterclockwise, and the clutch is plugged into the "chart" outlet. Thus, the clutch is engaged when the EUW-20A power switch is thrown to the "chart" position, causing the Digi-Pet and the chart paper to start at the same instant. The chart can be adjusted before the titration begins so that the pen rests directly on one of the chart lines. That point, easily located, will be the beginning of the titration. When the "function" switch is in the center or "standby" position, the motor is still turning counterclockwise but the clutch is disengaged so that the Digi-Pet is not delivering titrant. When the switch is in the right or "fill" position, the motor is turning clockwise and the clutch is engaged when the EUW-20A power switch is in the "Servo" position. In this position the piston in the Digi-Pet is being retracted, allowing the reservoir to be refilled. The delivery tube of the Digi-Pet is equipped with a

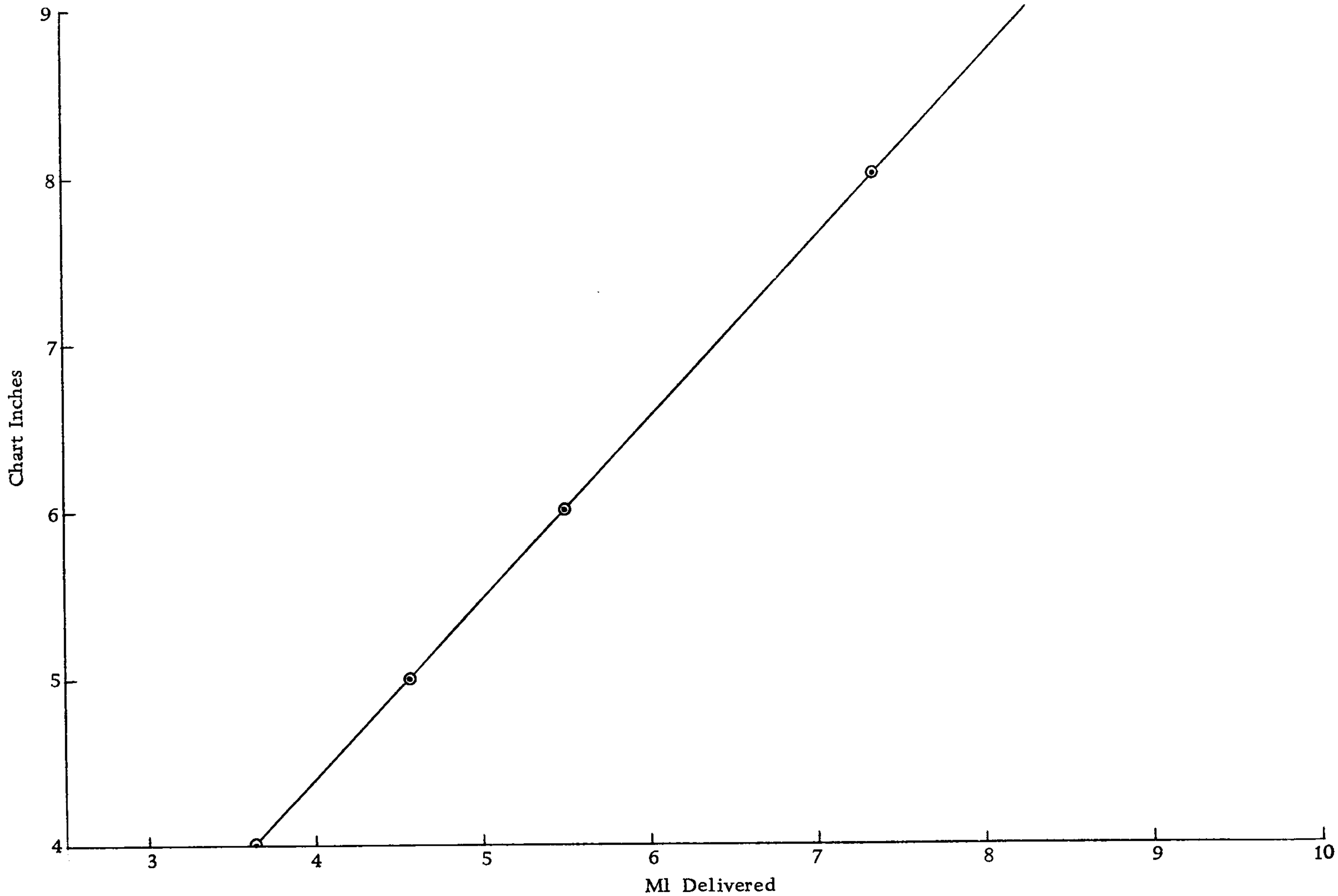

Figure 10. Chart inches versus ml delivered from Digi-pet.

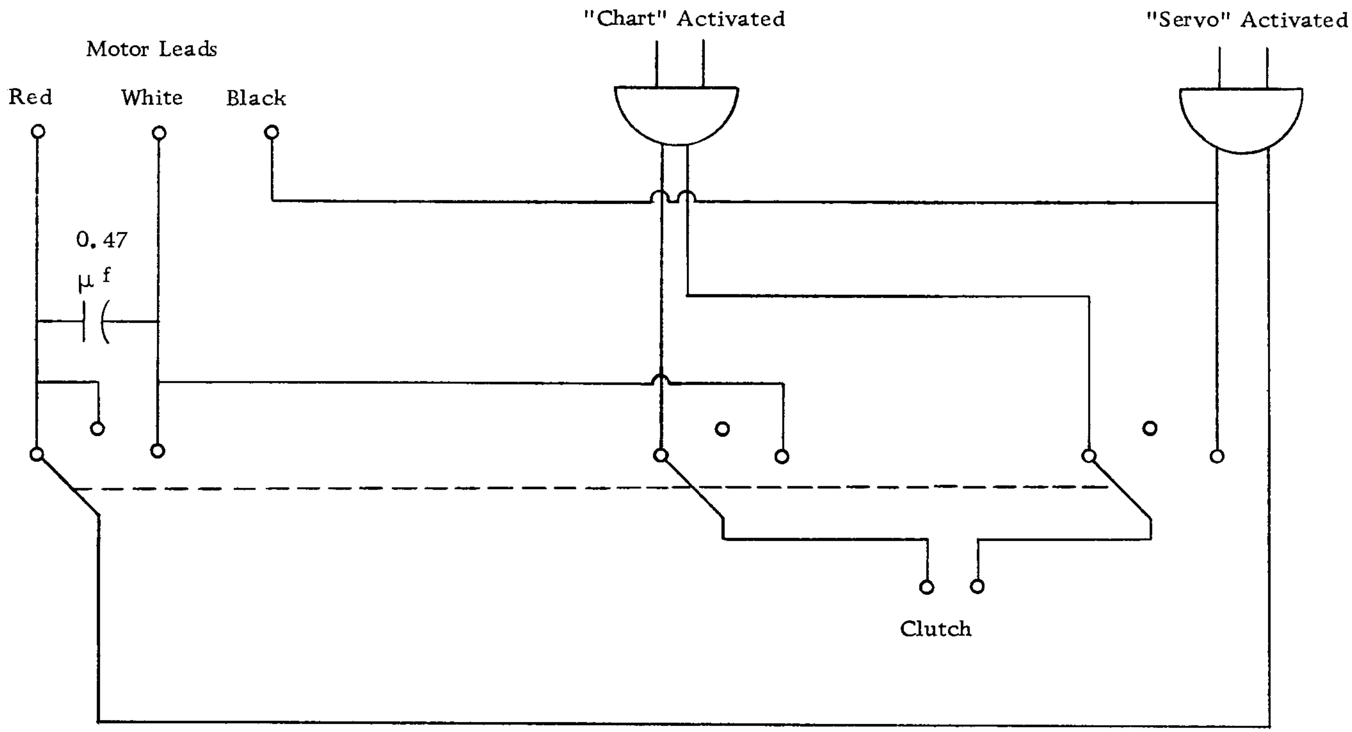

Figure 11. Function switch. Voltage, 115 v a-c, applied to the red and black motor leads causes counterclockwise turning. The motor is observed with the output shaft pointed toward the observer. The same voltage applied to the white and black leads causes clockwise turning. 115 v a-c applied to the two clutch leads causes the output shaft to turn in the above directions.

three-way stopcock as shown in Figure 12. During titration, the stopcock is positioned so that titrant is being forced from the reservoir out through the delivery tip by the advancing piston. During refilling, the stopcock is rotated so that the Digi-Pet reservoir is connected through the side tube to a large external reservoir filled with titrant. Then as the piston retracts, titrant is pulled into the Digi-Pet reservoir in preparation for a new titration. Up to this point, the Wheatstone bridge has been pictured as composed of purely resistive elements. Figure 9 shows that the instrument works very well under these circumstances. Unfortunately, a pair of electrodes dipping in an electrolyte solution is a combination of resistive and capacitive elements.

Conductance Cell

There is agreement on the nature of an electrolytic cell (5, 13). Figure 13 shows the electrical analog of a cell. R_1 is the bulk solution resistance, C_1 is the capacitance attributed to the ionic double layer around the electrodes, R_2 is a current path provided by the small amount of electrolysis which occurs at the surface of the electrodes, and C_2 is the sum of the "stray" capacitances between the electrodes and their leads. The admittances of R_2 and C_2 are usually small so a series combination of R_1 and C_1 is a good approximation of a cell. For a series RC

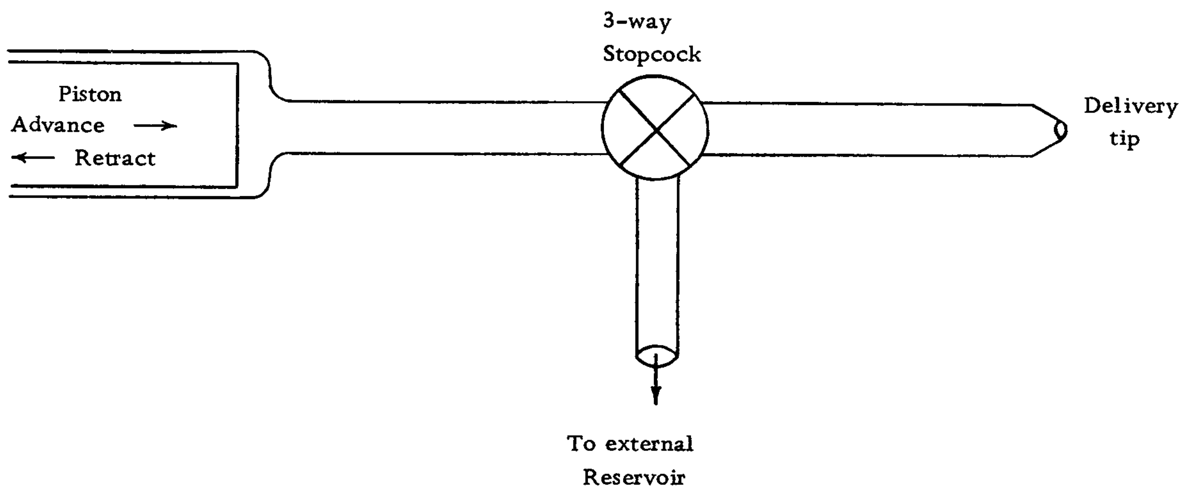

Figure 12. Digi-Pet delivery portion.

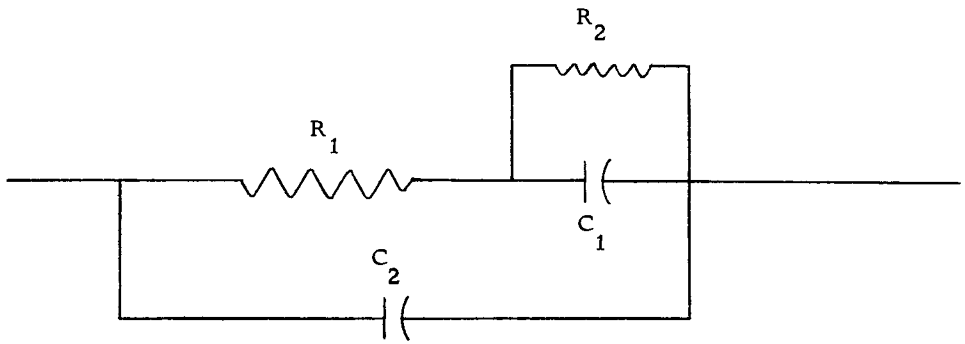

Figure 13. Electrical analog of a conductance cell.

combination, the phase angle, θ, between the applied potential and the current is given (10) by

$$\tan \theta = X_c/R = 1/(2\pi fRC) = L/(2\pi fC) \tag{15}$$

where f is the signal frequency and L is the solution conductance. Since L varies directly with solution concentration, M, a plot of M versus $\tan \theta$ should yield a straight line. Figures 14 and 15 are such plots. The data for these figures were obtained by immersing the previously described platinum wire electrodes in NaCl solutions and using this cell as R_3 in Figure 3. The phase angle was measured by connecting the ground lead of an oscilloscope to point 2, the vertical lead to point 4 and the horizontal lead to point 3. The phase angle was obtained from the resulting Lissajous figure in the conventional manner. It can be seen that in the range between 10^{-1} and 10^{-2}M NaCl the relationship is very nearly linear. Therefore, in the above concentration region, a series RC combination is a usable model of a cell to describe current voltage phase relationships. Since this project used concentrations in the 10^{-2}M NaCl vicinity, the above cell model will be used.

Reactive Bridge Analysis

A qualitative examination of a Wheatstone bridge containing the reactive cell described above proceeds as follows. The bridge

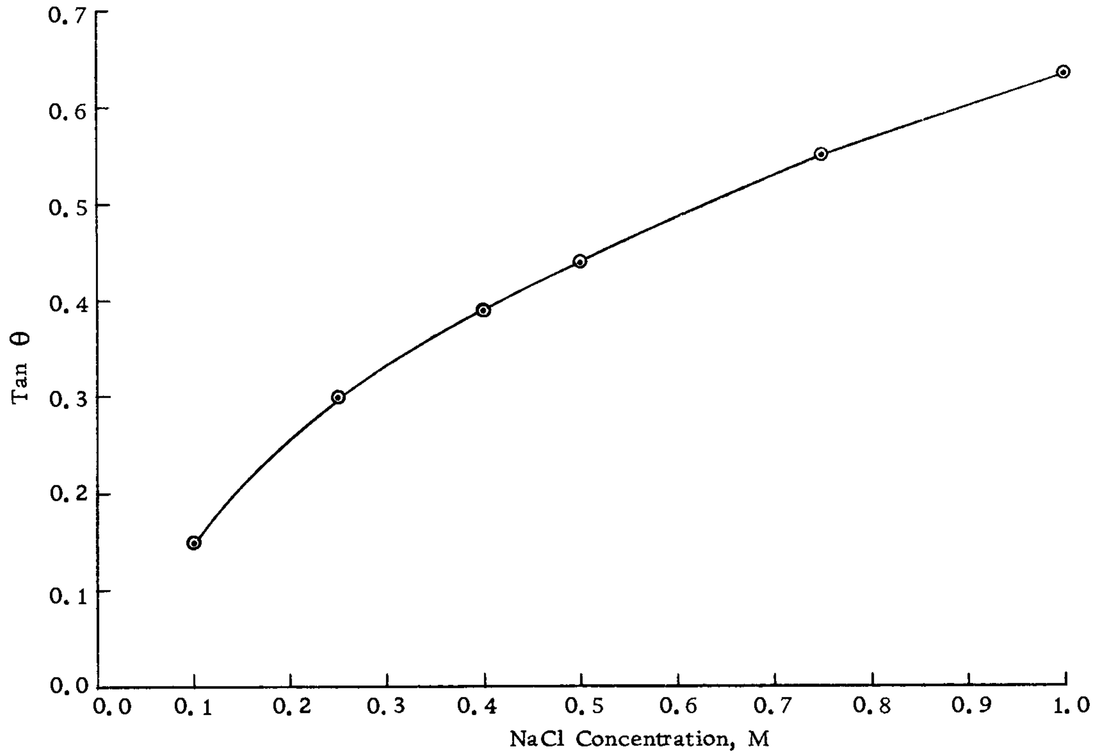

Figure 14. Concentration versus tan θ.

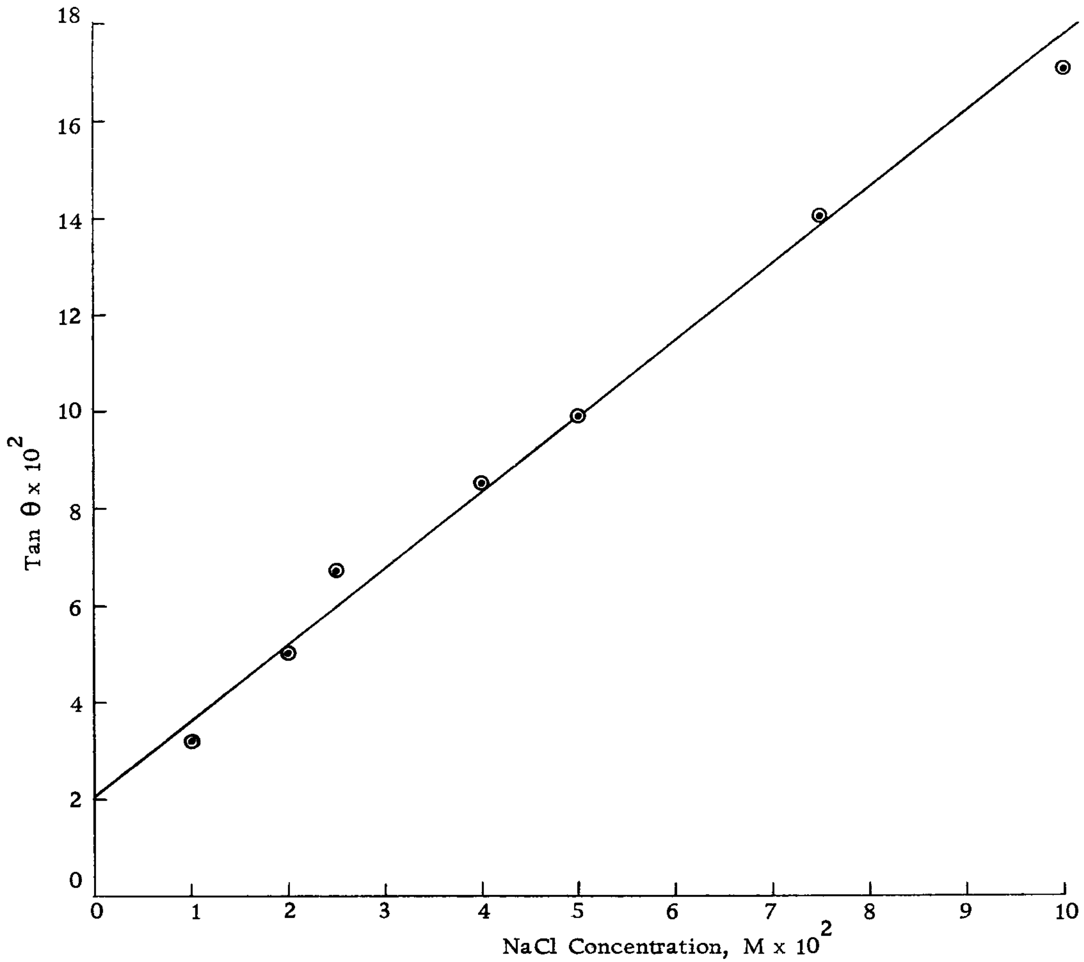

Figure 15. Concentration versus tan θ.

being considered is shown in Figure 16a, where the cell is represented by the arm CB and the variable resistor by arm AD. Figures 16b and 16c are polar coordinate representations of the various bridge potentials. The length of a vector represents the magnitude of a potential and the direction of a vector represents the phase relationship of a potential to the excitation potential. A vector representing the excitation potential would be placed in the conventional 0° position. The potential vectors for the left side of the bridge are shown in Figure 16b. With point C as the reference, the potentials across CD and across DA add to the signal potential CA as shown. These vectors are oriented in the conventional 0° position since they are both in phase with the excitation potential. As R_1 is increased, point D merely moves left along CA, and as R_1 is decreased, point D moves right. The potential vectors for the right side of the bridge are shown in Figure 16c. The potential across R_4, E_{cf}, and that across C_4, E_{fb}, add at right angles to form the resultant, CB. The potentials across R_3 and C_3 add in a similar manner to form BA. The angle θ is determined by the magnitudes of the elements in the right side. When 16b is superimposed on 16c (dotted line) it can be seen that under the conditions shown, the unbalance signal, DB,

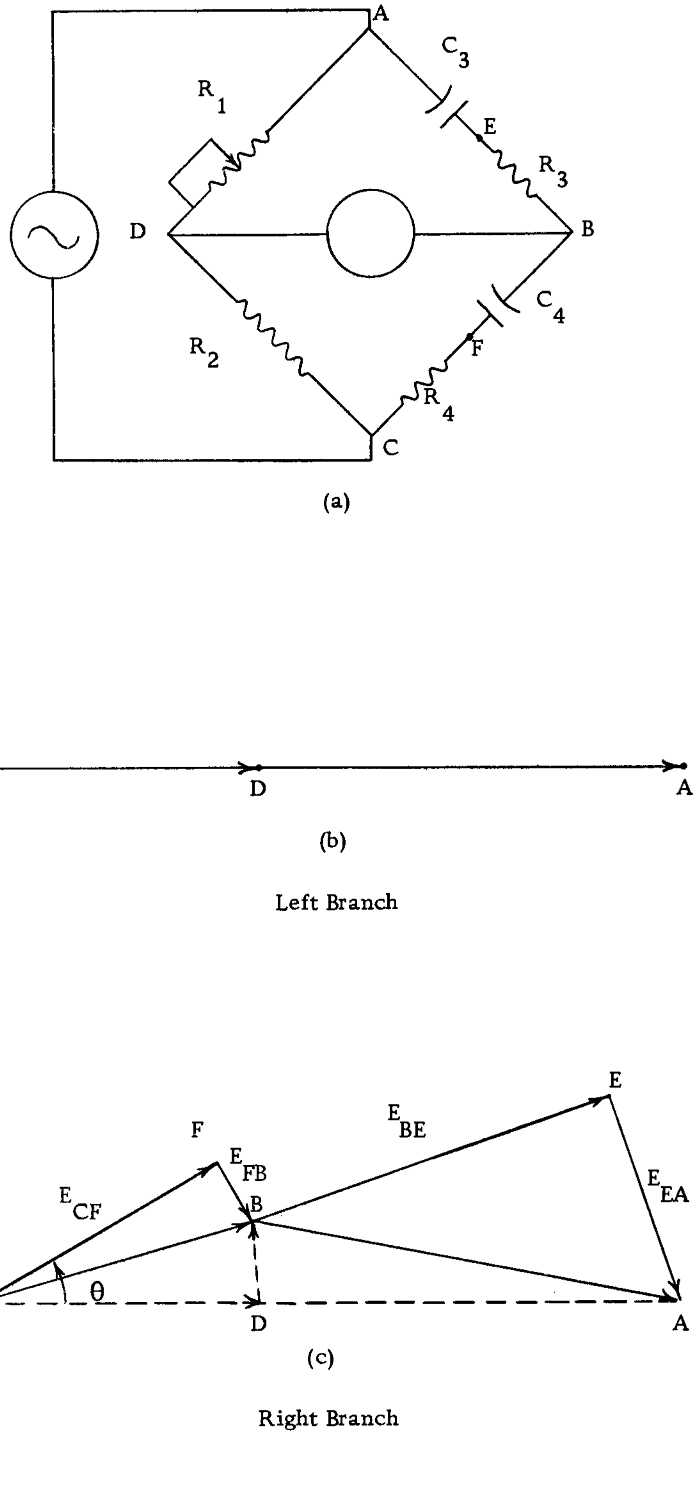

Figure 16. Reactive Bridge Potentials.

cannot be made zero by varying R_1. As R_1 is increased, D moves left and DB becomes a signal large in magnitude and shifted in phase a few degrees from CA. As R_1 is decreased, DB becomes a signal large in magnitude and shifted nearly 180^o from CA. If R_1 is adjusted so that DB has a minimum magnitude, it will be shifted in phase from CA by 90^o. This behavior is illustrated in the oscilloscope photo of Figure 17a. In each exposure of Figure 17, each major grid division on the horizontal scale represents 45^o. The smooth sine wave is the bridge excitation signal, and the rough wave is the unbalance signal. Although this photo was made with a parallel RC network in the upper arm of the right side of the bridge and a pure R in the lower arm, the unbalance signal behavior is the same as in the bridge of Figure 16a. In the top exposure, the bridge is unbalanced in one direction, in the bottom exposure it is unbalanced in the other direction, and in the middle it is brought as close to balance as possible by adjusting the variable resistor in the left side of the bridge.

To balance the bridge of Figure 16a, points D and B must be made to coincide. Adjustment of R_3 or C_3 can bring B down to vector CA where D can then be made to coincide with it by varying R_1. If R_4 varies, then point B follows a path which is a circle having its center on the perpendicular bisector

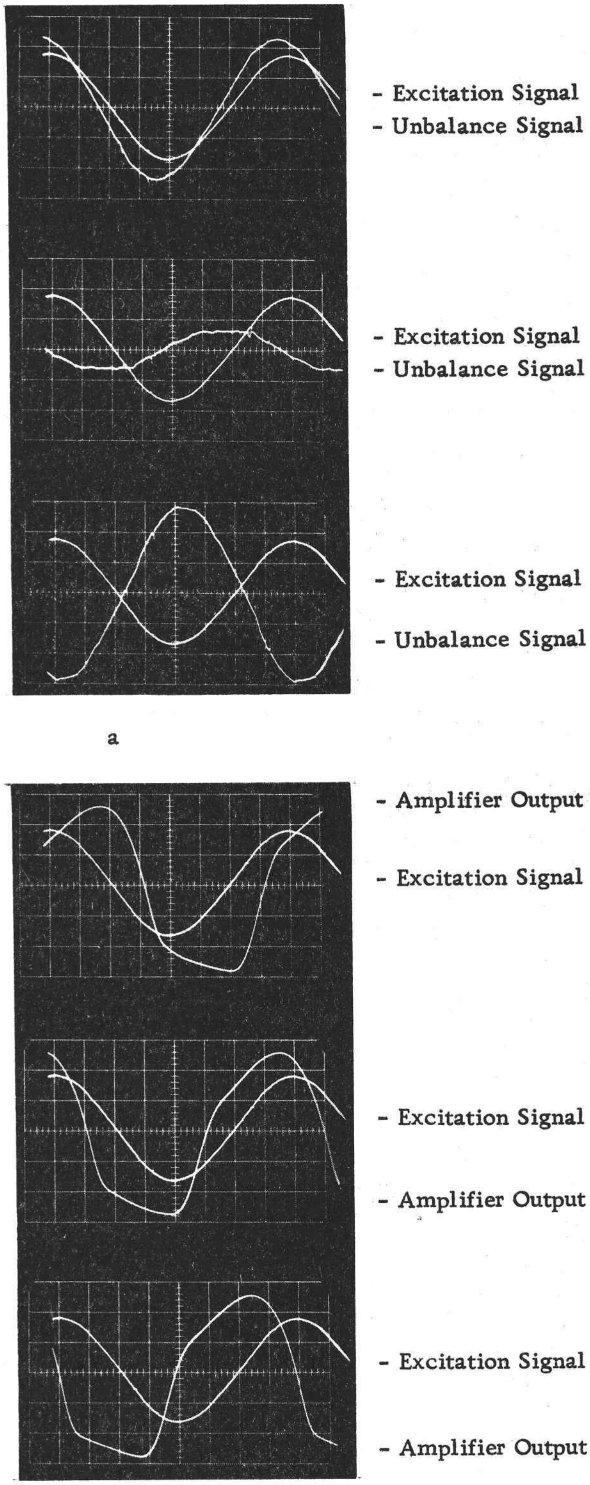

a

b

Figure 17. (a) Unbalance signals from reactive bridge.
(b) amplifier output for (a).

of DA and passing through points D and A (14). To re-balance the bridge after a change in R_4, either R_3 or C_3 must be re-adjusted to bring B back to vector CA. Therefore as R_4 varies during a titration, both R_1 and either R_3 or C_3 must be varied to keep the bridge balanced. Since the instrument used in this project had as the only controlled variable one of the resistors in the left side of the bridge, it is evident that a true bridge balance could not be maintained with this bridge. It is further evident that, as R_1 passed from one side of balance to the other, the unbalance signal varied from a large signal which was shifted a few degrees off zero to a small signal which was shifted 90° to a large signal which was shifted nearly 180°. The question which must be answered is: What effect does this phase shift have on the performance of the instrument?

The phase shift has no effect on the amplifier. It amplifies any a-c input, shapes it and shifts it 90°. Figure 17b shows the amplifier output signals for the inputs in 17a. The signal appearing at balance is an amplified hum, the cancellation of which is explained later. The performance of the servomotor, however, is phase-dependent. As stated previously, the signal at the control winding of the servomotor must be 90° out of phase with the reference winding to create the proper rotating magnetic field. To produce this phase relationship, the input signal to the amplifier must be either in phase with, or 180° out of phase with, the servomotor control winding, since any input signal is shifted 90° in the amplifier. If the excitation signal to a purely resistive bridge is in phase with the line signal, the proper phase relationship will occur at the servomotor windings, as shown previously. But we have seen that a reactive bridge yields an unbalance signal which is shifted in phase as much as 90° from the signal produced in a purely resistive bridge. An unbalance signal shifted 90° from the excitation (line) signal will produce a control winding signal either in phase with or 180° out of phase with the servo-motor reference winding (line) signal, because the unbalance signal undergoes an additional 90° phase shift in the amplifier. When the reference winding signal is in phase with or 180° out of phase with the control winding signal, there is no rotating magnetic field, and the servo-motor does not turn. The question asked above has now been reduced to a new one: How much phase error at the control winding will the servomotor tolerate?

Experiments Conducted

Phase Relationship Studies

The response of the servomotor to phase-shifted signals was studied in the following manner. Signals of various phases were produced with the network of Figure 18, and fed to the servoamplifier.

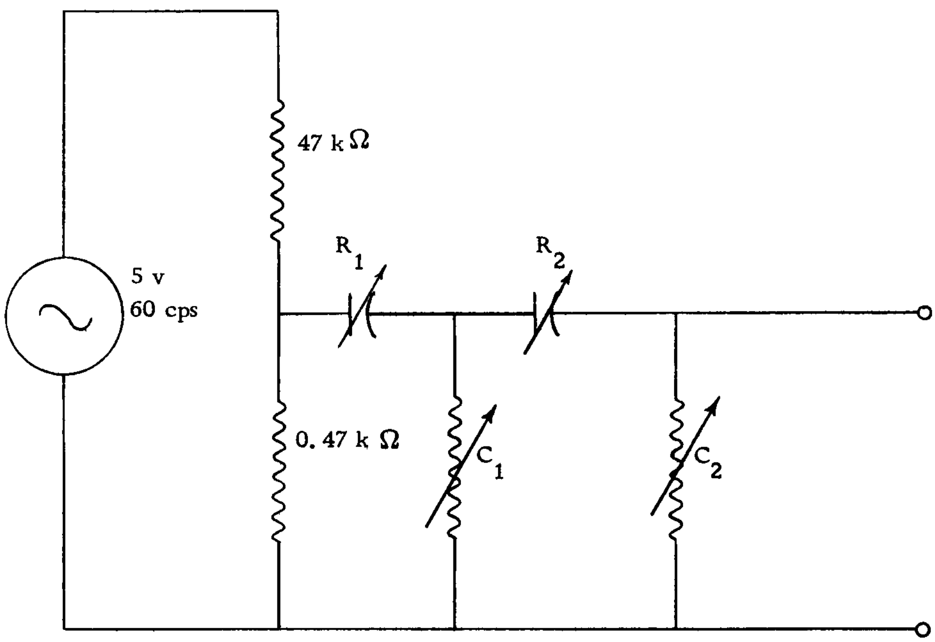

Figure 18. Phase shift network. R_1, R_2, C_1 and C_2 are decade boxes.

The amplifier output (Servo control winding) signal was displayed on one beam of the double-beam oscilloscope while the line (servo reference winding) signal was displayed simultaneously on the other. As the phase of the input signal was varied, the response of the servomotor was observed and pictures of the oscilloscope display were taken at the significant points. The pictures are shown in Figure 19a. The symmetrical sine wave is the line signal to the reference winding of the servomotor and the distorted wave is the signal to the control winding. In each photo mentioned below, the angle between the control and the reference was measured by estimating the number of major grid divisions between the peaks at the top of the photo. The number of major grid divisions multiplied by 45 degrees/division gave the angle in degrees. In photo 1, the control signal leads the reference by 90° and the servomotor is driving to the left. In photo 2, the control leads the reference by 130° and the motor is barely driving left. In photo 3 the control leads the reference by 155° and the motor is barely driving right. It drives right until photo 5, where the control leads by 305° and the motor barely moves. At photo 6, the control leads by 340° and the motor is barely moving left again. These data are presented graphically in Figure 19b. The vector labeled V_r represents the signal at the reference winding, oriented in the zero position. The other vectors in the figure represent the signal at the control winding,

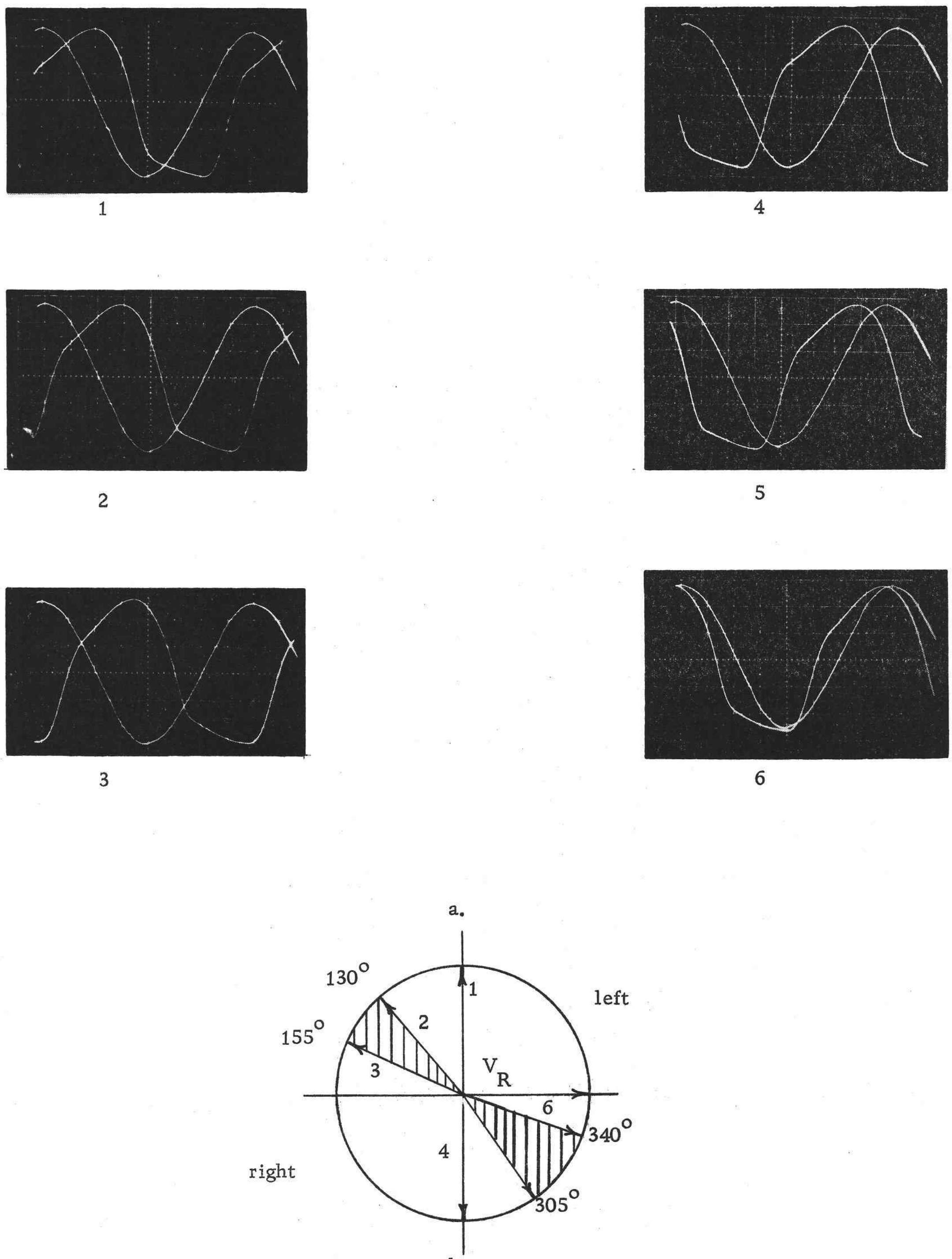

Figure 19. Phase relationships at servomotor.

oriented at various positions and numbered to correspond with the photographs. The darkened regions between 2 and 3 and between 5 and 6 are the regions where the motor does not turn, i.e., the dead band regions. In addition to the dead band regions, there are ill-defined regions on each side of these where the motor responds sluggishly.

The servomotor does not behave as expected--it seems that the dead bands should occur at 180° and 360°--but the fact remains that the unbalance signal from a reactive bridge passes through the dead band region when passing from one side of balance to the other. The questions to be answered now become: How serious is the effect of this dead band on titrations? and How can the dead band be reduced to a tolerable level?

Figure 16 shows that a relatively small angle between CB and AB can result in an unbalance signal which is shifted in phase from the excitation signal by angles ranging from a few degrees to nearly 180°. Furthermore, as the angle between CB and AB increases, the magnitude of DB cannot be made as small, and the angle between DB and CA will be greater at every setting of R_1. Therefore, the greater the angle between CB and AB the greater the range of settings of R_1 that will produce an unbalance signal in the dead band region of the servomotor.

To study the relationship of the angle between CB and AB to dead band, the following experiment was performed. The bridge of Figure 20 was constructed. R_3 was a decade resistance box which was accurate to 0.5%. C_3 was a set of capacitors, the capacitance of which had been measured with a Health Model 1B-2A Impedance Bridge which was accurate to three percent. The phase angle between AB and CB was calculated from

$$\text{Tan}\ \theta = R/X_c \tag{16}$$

Equation (16) gives the angle by which the current leads the potential in a parallel RC network (10). The current in AB will be in phase with the current in CB, since the current in each part of a current path is the same. Because CB is a non-reactive arm, its potential is in phase with its current. The potential across AB lags the current by the angle θ. Therefore the potential across AB lags the potential across CB by the angle θ. Measurements were made over a range from 10° to 0.2°. The dead band was measured by pushing the recorder pen off balance to the left until some driving force was encountered, releasing it, and letting it come to rest. After the rest position of the pointer was recorded, the pen was pushed to the right until force was encountered, released, and the rest position recorded. This sequence was repeated five times for each angle. The dead band reported was the distance between the rest points, averaged over the five measurements. The

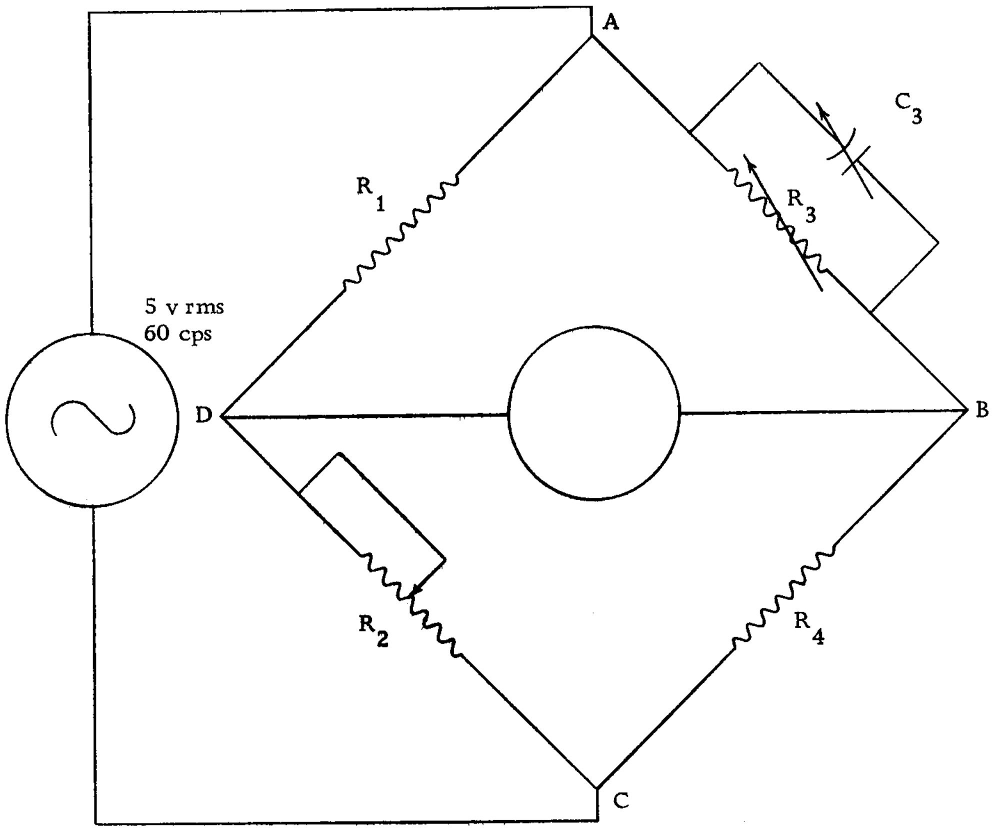

Figure 20. Reactive bridge used for phase shift versus dead band measurements.

data obtained are tabulated in Table 1 and plotted in Figure 21. It can be seen that the dead band is proportional to the phase angle, θ, between the potentials across AB and CB. It has been shown that the phase angle in an electrolytic cell increases with the electrolyte concentration. Therefore, the way to reduce dead band is to reduce electrolyte concentration.

Table 1. Relationship of the Angle Between CB and AB to Dead Band

Phase angle, degrees	Average Dead Band, Inches	Average Deviation, Inches
10	1.69	0.03
9	1.44	0.07
8	1.31	0.04
7	1.19	0.04
6	0.86	0.02
5	0.83	0.02
4	0.65	0.01
3	0.53	0.01
2	0.36	0.01
1	0.22	0.00
0.5	0.09	0.01
0.2	0.00	
0.1	0.00	

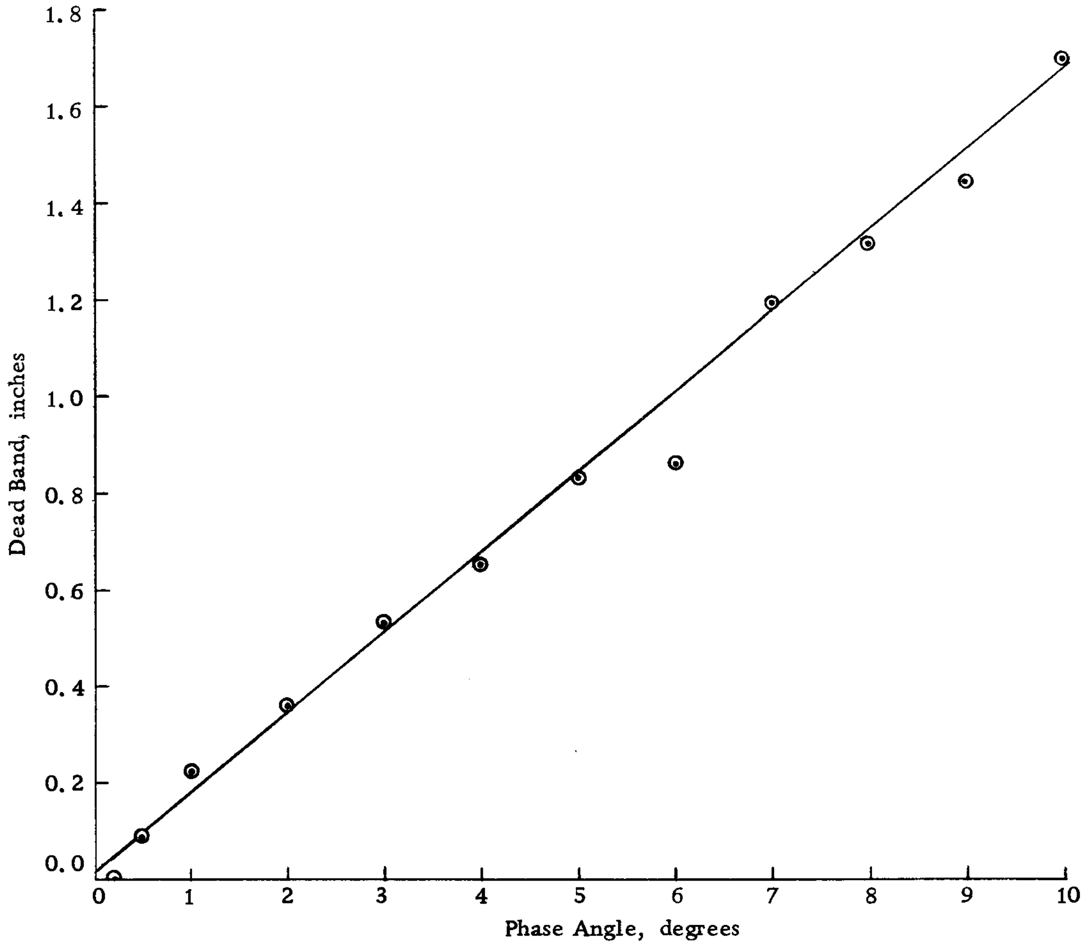

Figure 21. Bridge phase angle versus dead band.

Studies of Cell Conditions

During the work on this project, it was discovered that the conditions in the cell had a significant effect on the readout. A set of cell conditions which would produce the most usable readout was sought in the following manner. First, different types of stirring were studied. Since magnetic stirring is the type most commonly used in conductometric work, it was tried first. As the sensitivity of the instrument was increased, the stirring was found to cause regular oscillations of the pen with each revolution of the stirring bar. At this point, different types of stirring were tried in an effort to minimize the pen oscillation or chatter. Figure 22 shows the effects of three types of stirring on the pen chatter. These traces were made with the previously described platinum electrodes dipping in a solution of 0.01M NaCl. Figure 22a had an air-driven motor turning a glass rod which was spinning a glass disk 1.5 cm in diameter in the solution. The reason for using the glass disk was to move the solution by means of the continuous pull generated by the friction between the glass and the liquid rather than by the series of pushes resulting from the rotation of a stirring bar. It was hoped that this stirring would eliminate the repeated surges of solution past the electrodes and reduce pen chatter. Figure 22b had conventional magnetic stirring, and 22c had an electric motor driving a

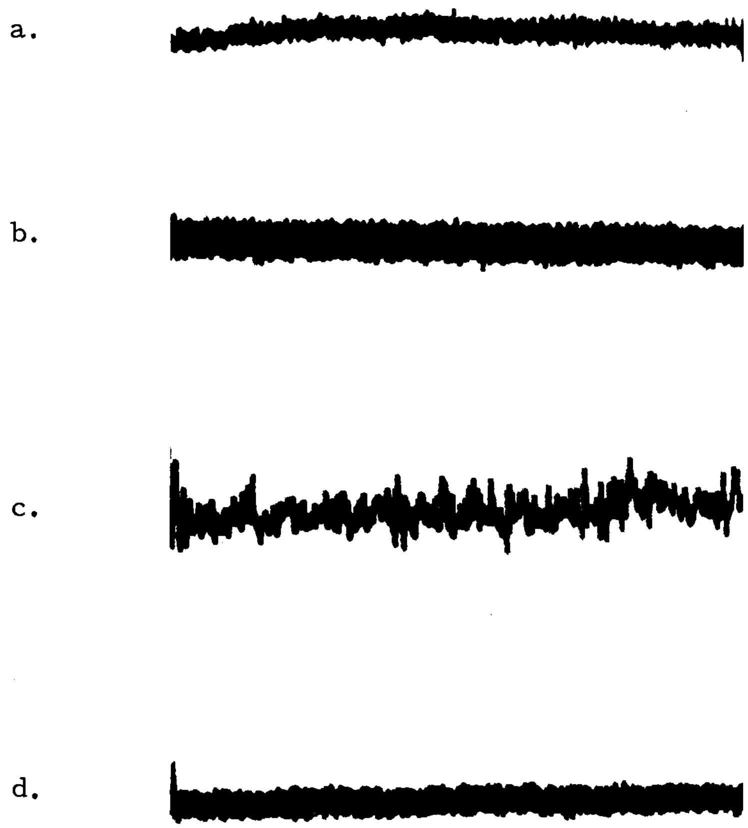

Figure 22. Effect of cell conditions on pen chatter. (a) air-driven glass disk (b) magnetic stirring (c) electrically-driven metal paddle (d) blacked Pt squares with magnetic stirring.

3-bladed stirring paddle on the end of a metal rod. Drawings of these stirrers are shown in Figure 23. Since pen chatter could not be eliminated, the stirring which produced the most constant amplitude and period and the best mixing was adopted. Magnetic stirring gave better chatter characteristics and better mixing, so it was used.

The stirring rate affected the pen chatter. Trial and error showed that a rate which resulted in a vortex approximately one cm deep gave the most uniform chatter. When the vortex or bubbles entered the region between the metal of the electrodes, the pen chatter became larger and more erratic.

The type of electrode used was also discovered to have an effect on the stirring chatter. Three different shapes of platinum electrodes were used, and each shape was tried when shiny and again when blacked to make a total of six different sets of electrodes. The three shapes were the previously described wires, heavy foil squares, 0.6 cm on a side and buttons which were 1.5 mm hemispheres. The trace produced by blacked wires with magnetic stirring is shown in Figure 22b. The blacked squares were used with magnetic stirring for the trace in Figure 22d. The same NaCl solution was used for all four parts of Figure 22. All three sets when shiny, and the buttons when blacked produced four-five inch dead bands with the instrument on five percent full scale sensitivity. The platinum wires were

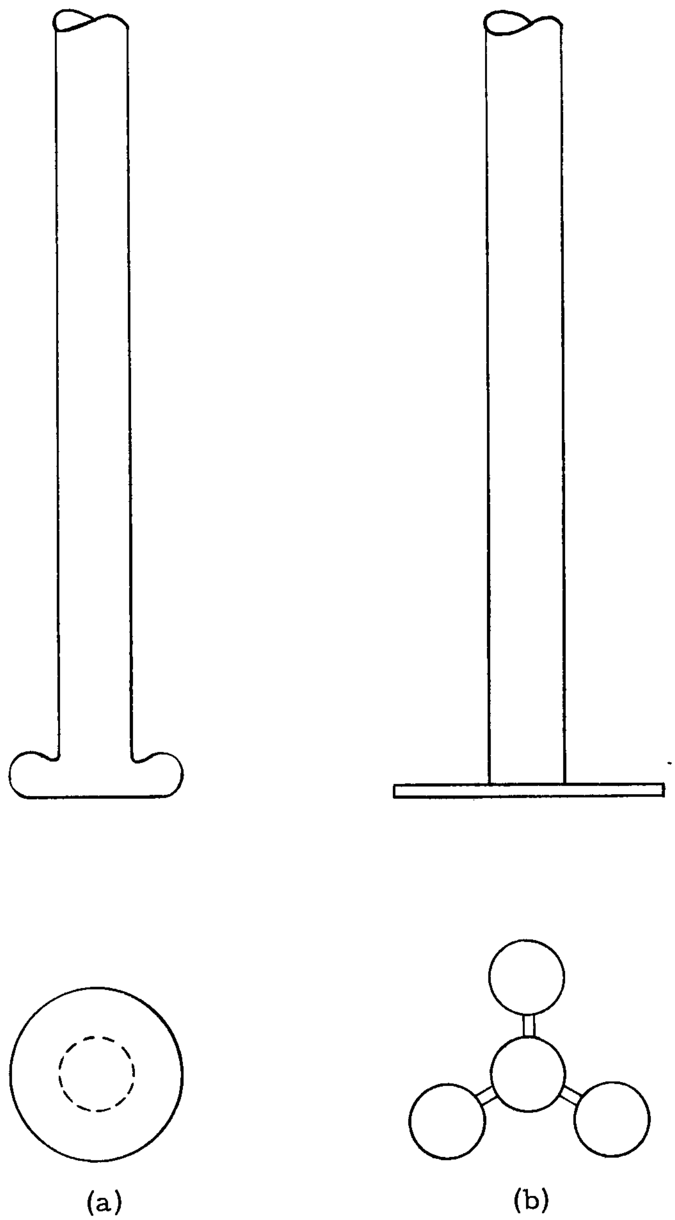

Figure 23. Stirring Rods. (a) air-driven glass rod
(b) electrically-driven metal paddle.

used for all titrations because they gave stirring characteristics as good as the squares and because they were more convenient to use and re-black. To achieve the best performance, it was found necessary to rinse the electrodes after each titration and to re-black them at the first sign of deterioration (6-10 titrations). The instrument's performance worsened--dead band increased--when any extraneous materials, e.g., towel fibers, caught on the electrodes. Once the best electrodes and stirring conditions were found, the instrument was evaluated by performing a series of titrations.

Titration Studies

For these studies, the instrument was arranged as in Figure 20 with a five volt rms 60 cps sine wave used to excite the bridge. The unbalance signal was fed to the servo amplifier and the slidewire of the EUW-20A was placed in the position of R_2 in Figure 20. Arm AB was the titration cell and a compensating capacitor was placed between R_4 and point B. Since point B is the ground side of the servo amplifier, the ground lead of an oscilloscope was attached there. The vertical plate lead was attached to point A and the horizontal to point C. The phase difference between the two arms produced an ellipse on the oscilloscope. Adjustment of R_4 reduced this ellipse to a straight line when the phases of the two arms became exactly 180° different. This phase adjustment was made at the beginning of the titration.

Because the gain of the EUW-20A servo-amplifier is approximately 10^6, a very small input signal will be amplified to the output limit of 105 volts. Extraneous signals, such as 60 cycle a-c picked up by induction from power supplies, are amplified along with input signals. To cancel these unwanted signals, referred to previously as "hum," the EUW-20A is equipped with a "hum adjust" potentiometer across the 6.3v filament supply as shown in Figure 24a. When the wiper is in the middle of the pot, no signal goes to the amplifier. When the wiper is toward one end, a signal of up to 3.15v is fed to the amplifier to cancel any 60cps signal that is in phase with line at that point in the amplifier. The amplifier input signal has by this time been shifted in phase a great deal. When the wiper is at the other end, the signal fed to the amplifier cancels any 60cps signal that is 180° out of phase with line. During this project the hum adjust built into the EUW-20A was found to be inadequate. It was replaced by a five kΩ pot across an external transformer, as shown in Figure 24b. This combination provided up to 20v on each side of zero and was found to be satisfactory. The effect of the hum adjust on the signal is shown in Figures 24c and 24d which were taken under the same conditions as 8b and 17b with the exception that the hum adjust was in use in the former and not in the latter.

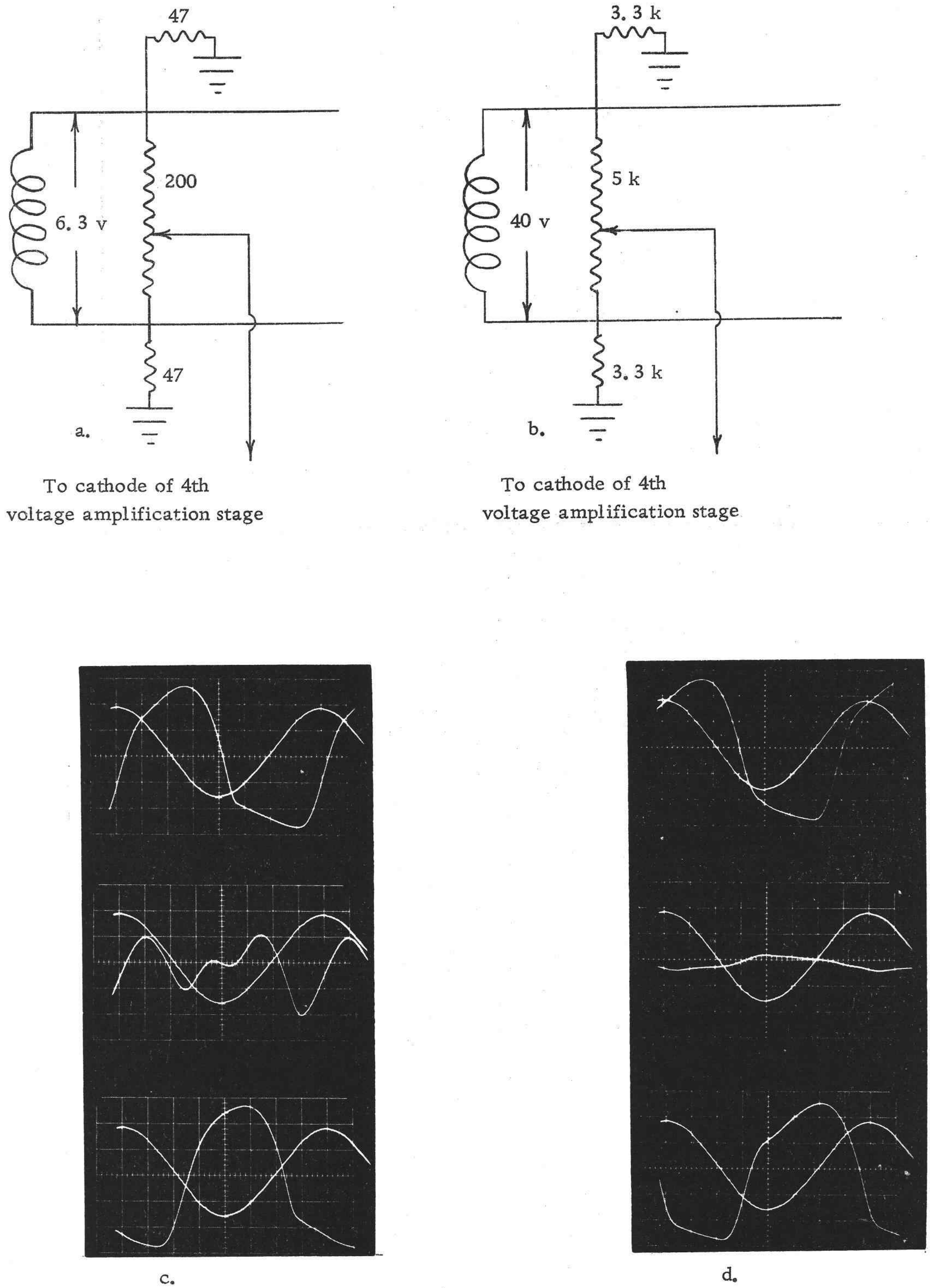

Figure 24. Circuits and effects of hum adjust.

The cell used in these titrations had blacked platinum wire electrodes with a cell constant of 1.0.

The yardstick used to evaluate a conductometric titrator is its ability to measure a small change in conductance. For this reason, the solutions titrated in this series were arranged to provide progressively smaller changes in conductance between the beginning of the titration and the endpoint. The systems were all Na_2CO_3 titrated with HCl. A strong acid-weak base titration provides the largest conductance change of any titration except for the strong acid-strong base type. Na_2CO_3 was used instead of a strong base to avoid the problem caused by CO_2 contamination of a strong base.

Figure 30 is an example of the titration of Na_2CO_3 with HCl. All the titration curves in this thesis begin at the right and proceed toward the left. At the beginning of this titration (point A), the principal ionic species present are Na^+, Cl^-, and $CO_3^=$. The Na^+ and Cl^- present remain in the solution and their contribution to the total conductance remains constant. The $CO_3^=$ ion is involved in the equilibrium

$$CO_3^= + H_2O \rightleftharpoons HCO_3^- + OH^- \quad (17)$$

During the early part of the titration, the addition of HCl increases the Cl^- concentration at a constant rate and converts $CO_3^=$ to

HCO_3^- according to the equilibrium

$$CO_3^{=} + H^+ \rightleftharpoons HCO_3^- \tag{18}$$

The increase of HCO_3^- concentration and corresponding decrease of $CO_3^{=}$ concentration resulting from the addition of HCl essentially eliminates the hydrolytic effect. The equilibrium expressed by equation (18) then controls the variation in conducting ionic species. Therefore, during the first inch of the curve, the conductance increase caused by increasing the concentration of Cl^- (Λ = 76.34 mho cm^{-1} equiv.$^{-1}$) is more than offset by the conductance decrease resulting from the decreased concentration of OH^- (Λ = 198 mho cm^{-1} equiv.$^{-1}$) and the conversion of $CO_3^{=}$(Λ = 69.3 mho cm^{-1} equiv.$^{-1}$) to $HCO_3^{=}$ (Λ = 44.5 mho cm^{-1} equiv.$^{-1}$). When a substantial amount of $HCO_3^{=}$ has been produced, the OH^- concentration becomes insignificant. The next two inches of the curve are dominated by the reaction

$$HCl + CO_3^{=} \rightarrow HCO_3^- + Cl^- \tag{19}$$

which results in the substitution of one HCO_3^- and one Cl^- for each $CO_3^{=}$, with little conductance change. When the level of $CO_3^{=}$ becomes low, the equilibrium

$$HCO_3^- + H^+ \rightleftharpoons H_2CO_3 \tag{20}$$

begins to appear. This reaction results in the substitution of a Cl^- for each HCO_3^- and a conductance increase. Reaction (20) is responsible for the linear portion extending from B to C on the chart. The endpoint of this titration (point C) occurs when all of the HCO_3^- has been converted to H_2CO_3. After the endpoint has been passed, the linear conductance increase is caused by the constant addition of H^+ (Λ = 350 mho cm^{-1} equiv.$^{-1}$) and Cl^- to the solution. The region between B and C and the region after C are extrapolated to their intersection at the endpoint.

In all titrations the concentration of the titrant was ten times that of the solution titrated to minimize dilution effects. To evaluate the performance of the instrument at different concentrations, Na_2CO_3 solutions having normalities of 10^{-1}, 10^{-2}, 10^{-3}, and 10^{-4} were titrated with HCl. The results are shown in the tables and charts of the next section. These titrations, while involving different concentrations, all gave the same percent change of conductance. To challenge the sensitivity of the instrument, the Na_2CO_3 solutions were modified by adding an inert electrolyte, NaCl. The NaCl initially present provided a constant conductance throughout the titration. The conductance change arising from the reaction between the Na_2CO_3 and HCl was therefore a smaller fraction of the total conductance than when no NaCl was present. By increasing the ratio of NaCl to Na_2CO_3, the conductance change was made progressively smaller.

When the solution being titrated had a total electrolyte concentration above 10^{-1}N, a dead band appeared as predicted in the section on phase relationships at the servomotor. The dead band could be reduced to zero at the beginning of the titration by adjusting R_4 until the potential of the R_4C_4 arm (arm CB) was exactly 180° from the potential of the cell arm (arm AB). As the titration progressed, however, and the cell characteristics changed, the dead band reappeared and made the titration unsatisfactory. An example of this phenomenon is included in the next section. When the solutions were made dilute enough, the dead band became sufficiently small that the titrations were satisfactory.

It has been reported (16) that a square wave has an advantage over a sine wave for conductometric titrations, i.e., that capitance compensation is unnecessary when a square wave is used. A square wave was generated with the circuit of Figure 25 and applied to the bridge in an effort to reduce the phase shift and resulting dead band. The same solutions were titrated as with the sine wave. The results of this series are contained in the next section.

Results

The results of the titrations described above are presented in tables two and three. The solutions used were all made by diluting

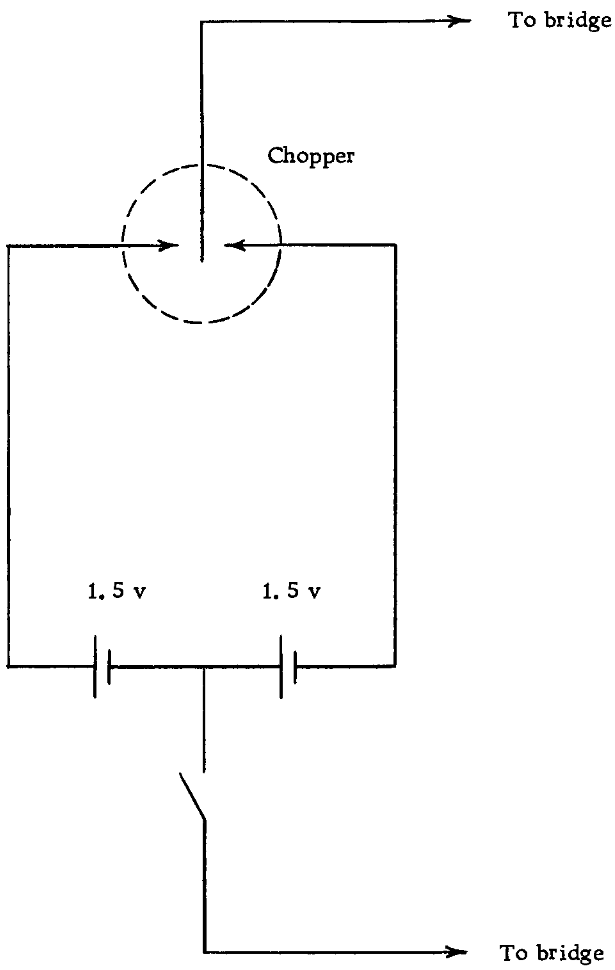

Figure 25. Square wave generator.

Table 2. Sine Wave Titrations of Na_2CO_3 with HCl

System #	Ml. HCl	Average Deviation %	Na_2CO_3 Normality Taken	Na_2CO_3 Normality Found	% Error	% Sensitivity
1	7.42 7.39 7.39	0.1	7.58×10^{-2}	7.55×10^{-2}	0.4	33.3
2	7.47 7.39 7.39	0.5	7.58×10^{-3}	7.57×10^{-3}	0.1	33.3
3	7.28 7.30 7.29	0.1	7.58×10^{-4}	7.44×10^{-4}	1.8	33.3
4	Dead band		7.58×10^{-5}			
5	7.33 7.32 7.37	0.3	7.58×10^{-3} 5×10^{-3} N NaCl	7.49×10^{-3}	1.2	20
6	7.36 7.41 7.37	0.3	7.58×10^{-3} 2×10^{-2} N NaCl	7.53×10^{-3}	0.6	10
7	7.36 7.38 7.38	0.1	7.58×10^{-4} 5×10^{-3} N NaCl	7.52×10^{-4}	0.8	7.5
8	7.23 7.32 7.34	0.5	3.79×10^{-4} 10^{-2} N NaCl	3.72×10^{-4}	1.8	5
9	7.29 7.24 7.29	0.3	7.58×10^{-4} 2×10^{-3} N NaCl	7.42×10^{-4}	2.1	10
10	7.45 7.47 7.45	0.1	7.58×10^{-3} 5×10^{-2} N NaCl	7.61×10^{-3}	0.4	5
11	7.30 7.46 7.42	0.8	3.79×10^{-3} 10^{-1} N NaCl	3.76×10^{-3}	0.8	5
12	Dead band		7.38×10^{-3} 0.25 N NaCl			5

Table 3. Square Wave Titrations of Na_2CO_3 with HCl

System #	Ml. HCl	Average Deviation %	Na_2CO_3 Normality Taken	Na_2CO_3 Normality Found	% Error	% Sensitivity
1	7.43 7.44 7.40	0.3	7.58×10^{-2}	7.57×10^{-2}	0.1	33.3
2	7.37 7.39 7.38	0.1	7.58×10^{-3}	7.53×10^{-3}	0.6	33.3
3	7.26 7.23 7.24	0.1	7.58×10^{-4}	7.38×10^{-4}	2.6	33.3
4	Dead band		7.58×10^{-5}			
5	7.41 7.40 7.42	0.1	7.58×10^{-3} 5×10^{-3} N NaCl	7.56×10^{-3}	0.3	20
6	7.39 7.37 7.38	0.1	7.58×10^{-3} 2×10^{-2} N NaCl	7.53×10^{-3}	0.6	10
7	7.33 7.32 7.33	0.0	7.58×10^{-4} 5×10^{-3} N NaCl	7.48×10^{-4}	1.3	7.5
8	7.38 7.33 7.43	0.4	3.79×10^{-4} 10^{-2} N NaCl	3.76×10^{-4}	0.8	5
9	7.32 7.26 7.25	0.4	7.58×10^{-4} 2×10^{-3} N NaCl	7.43×10^{-4}	2.0	10
10	7.38 7.43 7.47	0.4	7.58×10^{-3} 5×10^{-2} N NaCl	7.58×10^{-3}	0.0	7.5
11	Dead band		3.79×10^{-3} 10^{-1} N NaCl			

stock solutions of HCl and Na_2CO_3. The stock HCl solution was standardized potentiometrically against weighed samples of Na_2CO_3. The Na_2CO_3 stock solution was then standardized against the HCl stock solution. The instrument used in all standardizations was the Heath pH Recording Electrometer. The HCl stock solution was found to be 1.02 N and the Na_2CO_3 stock solution was found to be 0.758 N. In every titration the HCl solution was approximately 10 times more concentrated than the Na_2CO_3 solution, e.g., in system one, 0.0758 N Na_2CO_3 was titrated with 1.02 N HCl. The Na_2CO_3 normality taken is the normality of the diluted stock solution and the normality found is the normality resulting from the conductometric titration. The ml HCl values were obtained by reading the number of chart inches from the beginning of the titration to the endpoint and converting the resulting numbers to ml by using Figure 10. The percent average deviation value for each system is the arithmetic mean of the deviations of the three ml HCl values from the average ml HCl value. The percent error is the percent difference between the normality of Na_2CO_3 taken and the normality of Na_2CO_3 found. The percent sensitivity column refers to the sensitivity of the instrument and means the percent conductance change which will move the pen full scale.

In addition to the numerical results, several observations were made on the performance of the instrument:

(1) When using either the sine wave or the square wave, the maximum usable sensitivity of the instrument is five percent. Titrations attempted with a two percent sensitivity showed a dead band of 0.3" or more. A dead band that large results in an unsatisfactory titration.

(2) Dilution of the solutions improved the performance of the instrument with a sine wave. The titration curves of Figures 26 and 27 were both made with the instrument on five percent sensitivity. Figure 26 had a total electrolyte concentration of 0.26 N and Figure 27 had a total electrolyte concentration of 0.06 N. In Figure 26 the dead band was zero at the beginning, but it soon increased until the instrument response was too sluggish to give a usable curve. In Figure 27 the dead band also increased during the titration, but the curve was still usable.

(3) Dilution of the solutions also improved the instrument performance with a square wave. Figure 29 shows the distortion of the square wave caused by increased electrolyte concentration. When the total electrolyte concentration was 0.1 N or above, square wave titrations could not be performed.

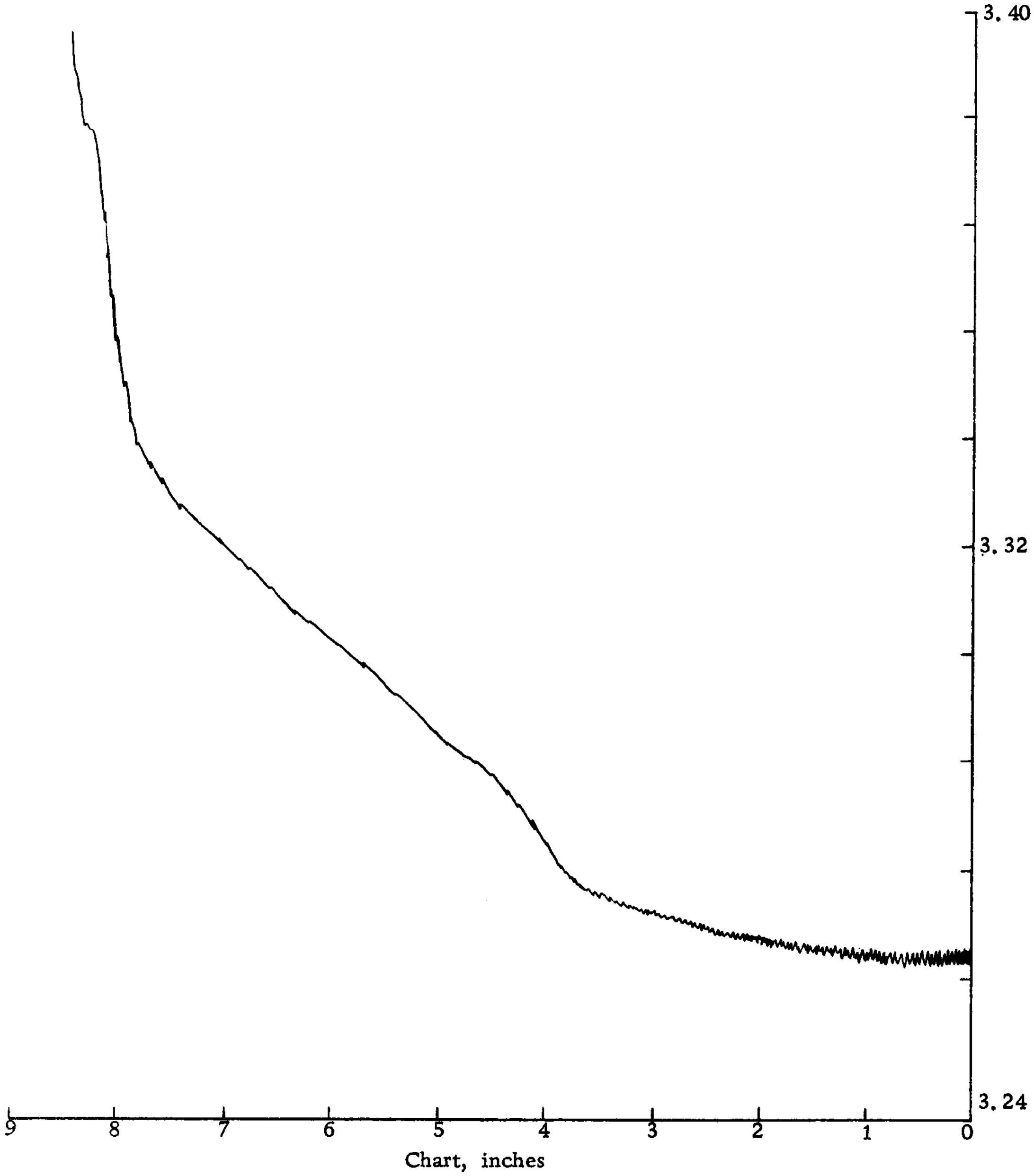

Figure 26. Sine-wave titration of 10^{-2} N Na_2CO_3 in 0.25 N NaCl. Sensitivity equals 5%.

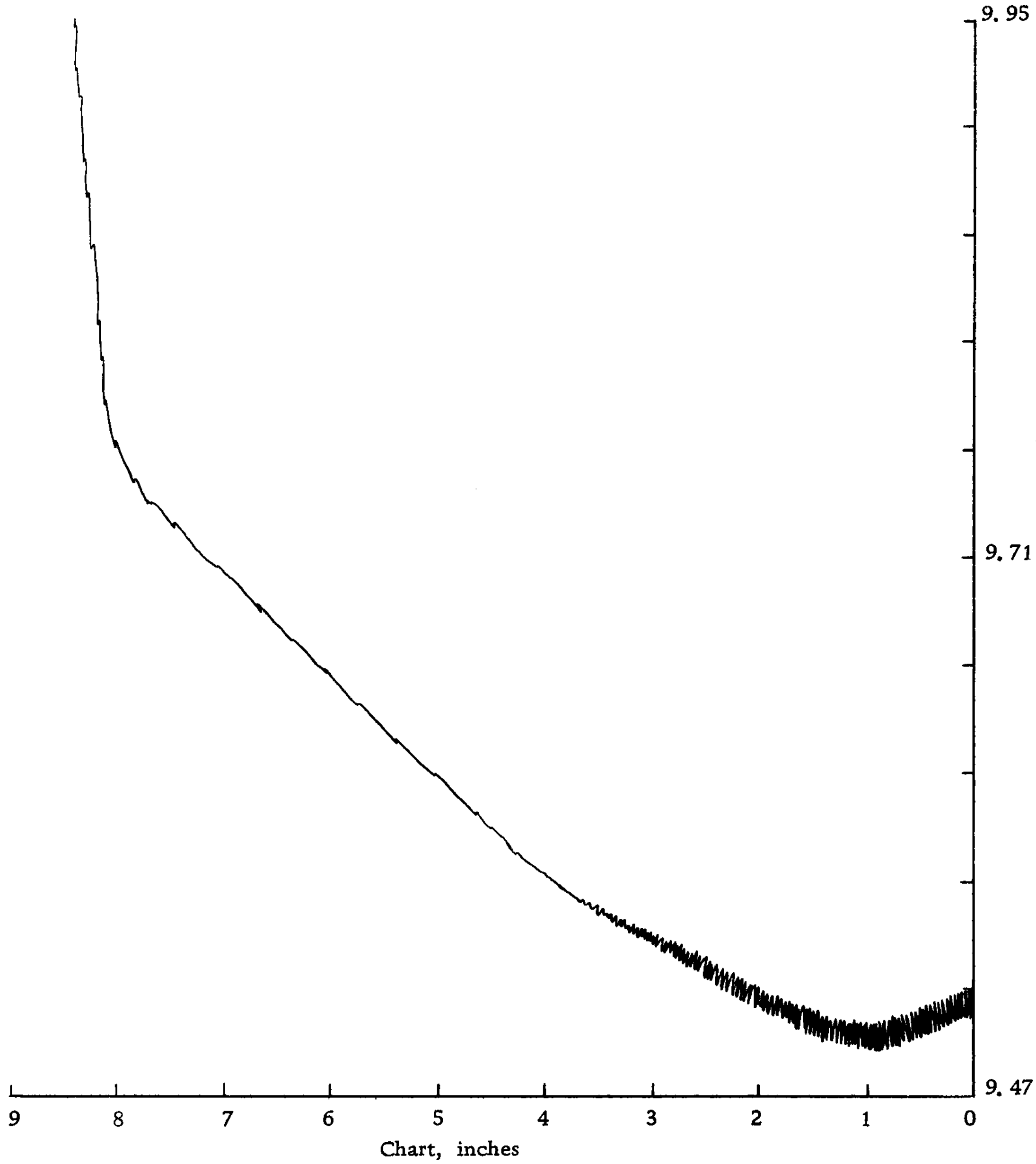

Figure 27. Sine-wave titration of 10^{-2} N Na_2CO_3 in 5×10^{-2} N NaCl. Sensitivity equals 5%.

(4) Capacitance compensation had no effect on the square-wave instrument performance. For this reason, no capacitance was used during the square-wave titrations.

(5) The dead band could be eliminated at any point in the sine-wave titrations by inserting a compensating capacitor between R_4 and point B of Figure 20 and adjusting R_4. During the course of the titration, however, the phase shift and the dead band returned as shown in Figure 28.

(6) A titration takes approximately ten minutes with this instrument including the time to refill the Digi-Pet.

(7) The titrant must have the same concentration of inert electrolyte as the solution titrated or dilution will cause a large conductance change during the titration.

(8) In several instances the square wave gave a more satisfactory curve than the sine wave. Figure 30 is a square-wave titration and Figure 31 is a sine-wave titration of the same system with all other conditions identical.

Discussion

The data presented in Tables 2 and 3 show little difference between the performance of the instrument with a sine wave and that with a square wave, with one exception: the sine wave

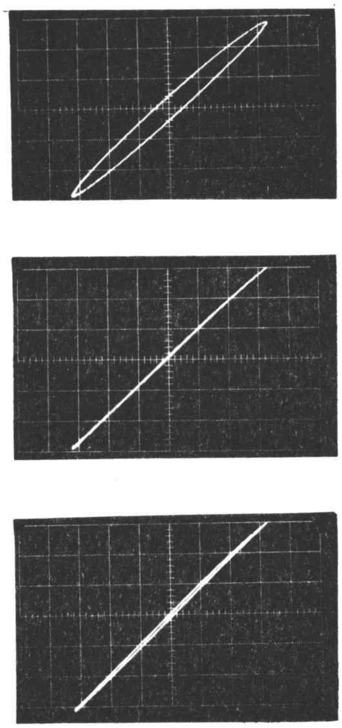

Figure 28. Phase shift during titration. Top exposure shows 10^{-2} N NaOH in 10^{-1} N NaCl with no capacitance compensation. Second exposure shows same solution with 20 μf in the bridge. Third exposure shows the same solution after titration with 10^{-1} N HCl in 10^{-1} N NaCl.

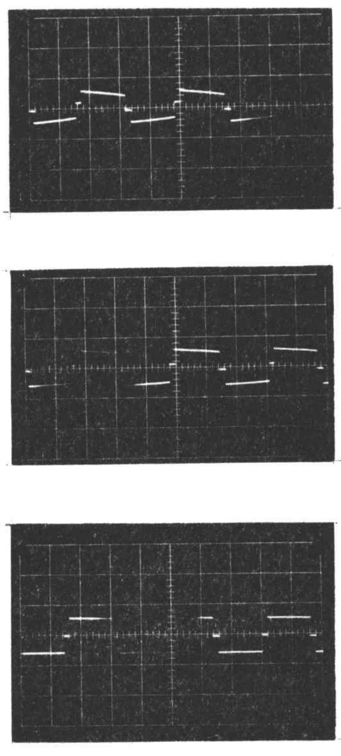

Figure 29. Effect of concentration on square wave. Top exposure shows the potential across the cell with 10^{-1} N NaOH in it. Second exposure shows effect of 5×10^{-2} N NaOH and third exposure shows 1×10^{-2} N NaOH.

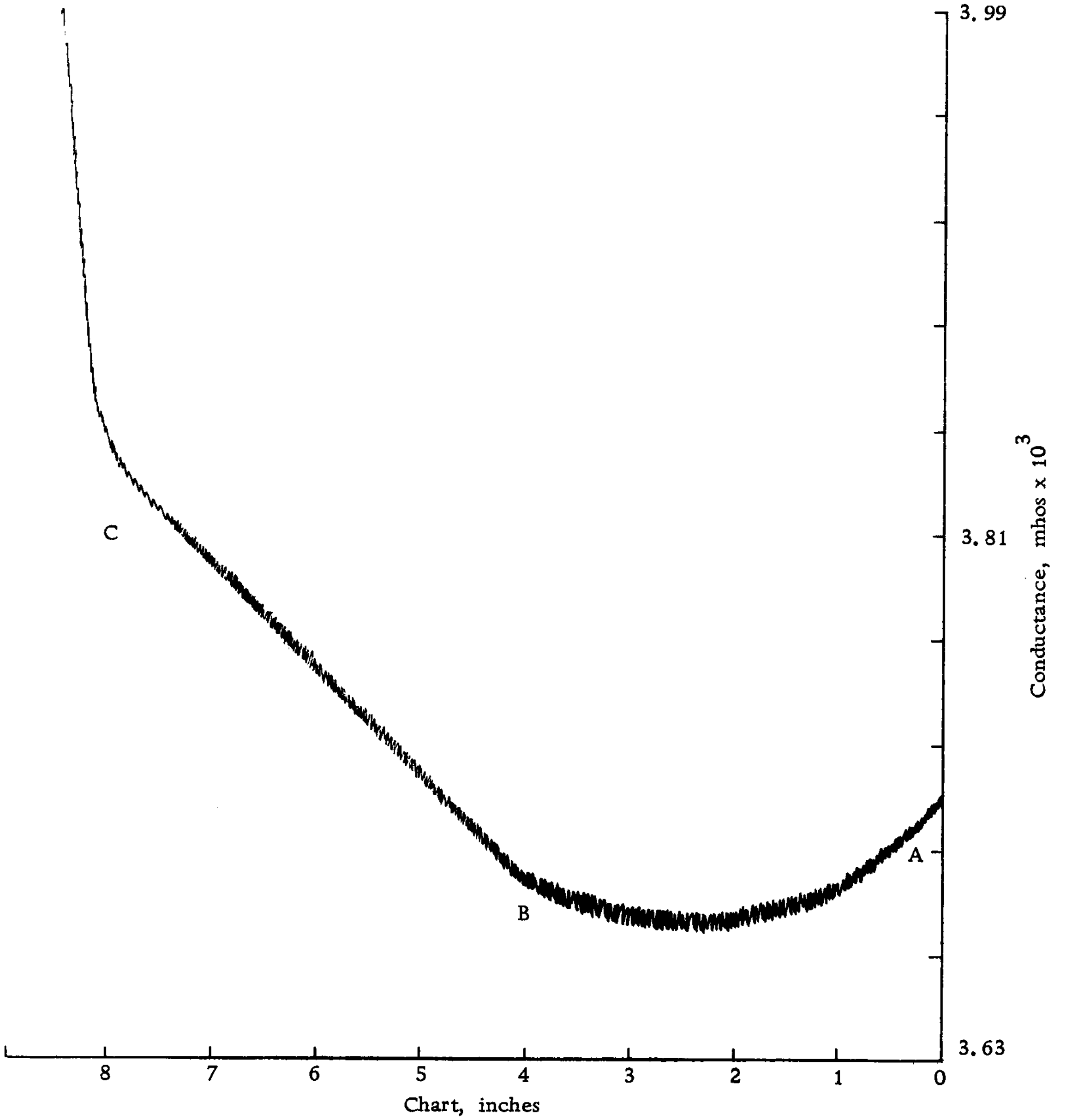

Figure 30. Square-wave titration of 10^{-2} N Na_2CO_3 in 2×10^{-2} N NaCl. Sensitivity equals 10%.

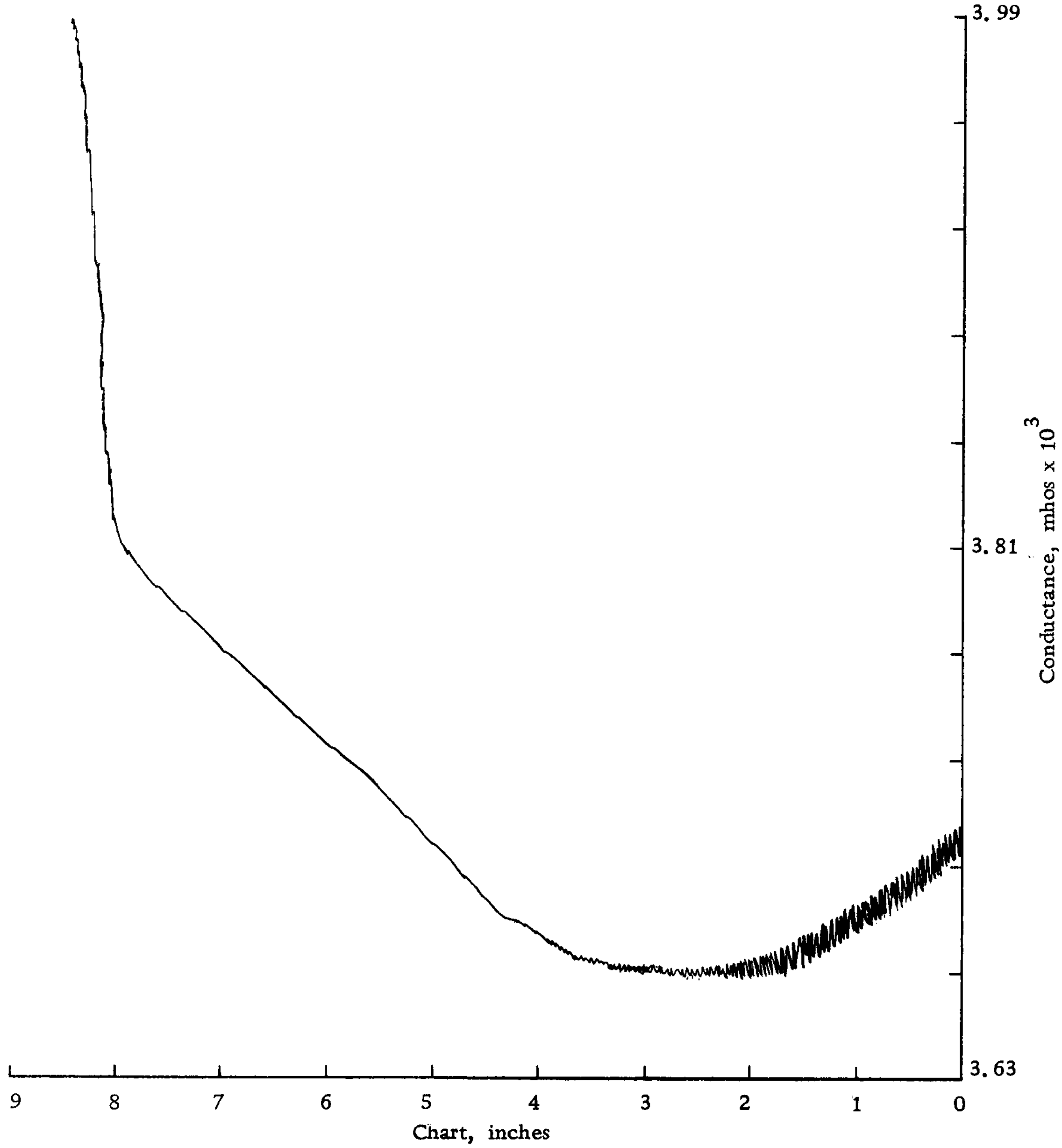

Figure 31. Sine-wave titration of 10^{-2} N Na_2CO_3 in 2×10^{-2} N NaCl. Sensitivity equals 10%.

instrument gave satisfactory results for system 11 while the square wave could not titrate it. In accordance with observation (3) above, system 11 is too concentrated for a square-wave titration. With the sine wave, the effect of this high concentration, phase difference between two bridge arms, can be minimized by capacitance compensation and the titration can be performed. The solution of system 12, however, was found to be too concentrated for a sine wave titration. A one-half inch dead band appeared shortly after the beginning of this titration.

The square wave instrument is more convenient since it requires no external transformer, no compensating capacitors, and no oscilloscope to achieve capacitance compensation. With the square wave, the bridge is more flexible because the resistor between points C and B in Figure 20 can be varied to achieve initial balance. With the sine wave, this resistor is adjusted initially to achieve exactly 180° phase difference between arms AB and CB after which it cannot be changed. Initial bridge balance must be secured by adjusting R_1.

The reproducibility of the results is good, with average deviations for all systems but one being one-half percent or less. Because the total titration requires less than ten inches of chart paper, an average deviation of one-half percent represents 0.05 inches of chart paper. When these extrapolated endpoints show a deviation this small, the reproducibility can be considered good. Of the 19 conductometric determinations of Na_2CO_3 normality, 12 determinations showed errors of less than one percent. Of the seven determinations having errors greater than one percent, six involved the titration of Na_2CO_3 solutions less concentrated than 10^{-3} normal, and each of these six gave a low result. A possible explanation for these low results arises from two characteristics of the titration curve. The Na_2CO_3 solutions which were less concentrated than 10^{-3} normal produced long, rounded curves in the endpoint region. Because the conductance increased rapidly in the region after the endpoint, the pen went off scale within the first inch after the endpoint. Since a part of this inch was included in the rounded endpoint region, the post-endpoint region covered less than an inch of the chart. When the post-endpoint region of the curve is relatively short, it is difficult to determine where the endpoint region ends and the post-endpoint region begins. Thus the portion which is extrapolated could include part of the endpoint region with the result that the extrapolated line would not be steep enough and the endpoint would occur early.

CONCLUSION

The Heath EUW-20A Servo-Recorder, in modified form, is a useful conductometric titrator. The restrictions accompanying its use are that it cannot be used in highly concentrated solutions and that it cannot perform a titration which requires a sensitivity of more than five percent. For most titrations, a square wave is superior to a sine wave for exciting the bridge both because it is more convenient to use and because no loss of sensitivity occurs during the titration. Solutions titrated with this instrument must be as dilute as possible, to decrease distortions of the bridge signal.

The good reproducibility demonstrated by this instrument makes it suitable for routine control analyses, where relative rather than absolute values are important. It might also be suitable for educational applications because of its ease of construction and simplicity.

BIBLIOGRAPHY

1. Anthony, Anton and Paul W. Mullen. A universal automatic recording titrator. Talanta 8:817-823. 1961.

2. Boardman, W. A full scale automatic conductance titrimeter. Chemistry and Industry, April 6, 1963, p. 565-567.

3. Colvin, D. W. and R. C. Propst. A recording conductometric titrator. Analytical Chemistry 32:1858-1861. 1960.

4. Ewing, Galen W. and Thomas H. Brayden, Jr. The Heath Analog Computer as a versatile analytical tool. Analytical Chemistry 35:1826-1828. 1963.

5. Feates, F. S., D. J. G. Ives and J. H. Pryor. Alternating current bridge for measurement of electrolytic conductance. Journal of the Electrochemical Society 103:581. 1956.

6. Goodwin, Robert Daniels. Automatic recording of carbon dioxide by conductometry. Analytical Chemistry 25:263-265. 1953.

7. Heath Company. Operation manual for the Malmstadt-Enke Instrumentation Laboratory Station. Benton Harbor, Michigan, n.d. Various paging. (EUW-20A section)

8. Holm-Jensen, I. B. Automatic recording in conductometric precipitation titration of carbon dioxide. Analytica Chimica Acta 33:198-204. 1965.

9. Juliard, A. and J. Van Cakenberghe. Automatic conductometric titration. Analytica Chimica Acta 2:542-544. 1948.

10. Malmstadt, H. V., C. G. Enke and E. C. Toren, Jr. Electronics for scientists. New York, Benjamin, 1963. 581 p.

11. Maron, Samual H. and Carl F. Prutton. Principles of physical chemistry. New York, Macmillan, 1958. 771 p.

12. Morrison, Charles F. A practical instrument synthesizer. Analytical Chemistry 35:1820-1826. 1963.

13. Mueller, T. R., R. W. Stelzner, D. J. Fisher and H. C. Jones. High-sensitivity, direct-reading, linear, recording conductometric titrator with automatic temperature compensation or proportional temperature control. Analytical Chemistry 37:13. 1965.

14. Stout, Melville B. Basic electrical measurements. New York, Prentice-Hall, 1950. 479 p.

15. Walisch, W. and J. Barthel. Accurate measuring of small electrolytic resistances with a new type of immersion cell, in accordance with the phase-shift method. II. An automatic conductivity bridge with digital indication. Zeitschrift für Physikalische Chemie, Frankfurt (West Germany) 39:235-240. 1963.

16. Wijnen, M. D., A. B. Ijzermans and J. H. Schmieman. Square wave conductometry. Recueil des Travaux Chimiques des Pays-Bas 83:21-30. 1964.